

# JOURNAL OF BIOMEDICINE AND TRANSLATIONAL RESEARCH

Available online at JBTR website: <https://jbtr.fk.undip.ac.id>

Copyright©2024 by Faculty of Medicine Universitas Diponegoro, Indonesian Society of Human Genetics and Indonesian Society of Internal Medicine

Original Research Article

## Complex interaction between allopurinol-induced uric acid reduction and glycemic control: a clinical and molecular study

Lucyana Pongoh<sup>1</sup>, Jonesius Eden Manoppo<sup>1</sup>, Gerry Supit<sup>2</sup>, Alva Supit<sup>1\*</sup>

<sup>1</sup>Department of Public Health, Universitas Negeri Manado, Indonesia

<sup>2</sup>Emergency Department, Sam Ratulangi General Hospital, Indonesia

### Article Info

History

Received: 29 Feb 2024

Accepted: 09 Dec 2024

Available: 30 Dec 2024

### Abstract

**Background:** Diabetes mellitus type 2 (DMT2) and hyperuricemia are two prevalent metabolic diseases worldwide, including in Indonesia. Within the Minahasa tribe, the prevalence of these diseases is among the highest in Indonesia. The interaction between hyperuricemia and DMT2 is inconclusive, as previous studies about whether allopurinol and its related uric acid reduction correlate with insulin resistance have shown conflicting results.

**Objective:** To examine whether allopurinol-induced uric acid reduction can modify insulin resistance in nondiabetic Minahasan male subjects and to study the putative molecular mechanisms of this interaction.

**Methods:** The clinical part of this research was a pseudo-experiment with a pre-test/post-test design. Twenty nondiabetic Minahasan male subjects were subjected to the daily dose of 300 mg allopurinol for three months. Plasma glucose, uric acid, and insulin levels were measured pre- and post-treatment. Homeostatic model assessment of insulin resistance (HOMA-ir) values was calculated by the Oxford HOMA calculator. For the wet lab experiment, the human embryonic kidney HEK293T cell line was treated tolerable allopurinol concentrations. The expression of glucose transporter 4 (*GLUT4*), glucose transporter 1 (*GLUT1*), insulin receptor isoform A (*IR-A*), and thioredoxin-interacting protein (*TXNIP*) mRNAs were analyzed by quantitative real-time polymerase chain reaction (qPCR).

**Results:** In nondiabetic Minahasan male subjects, allopurinol administration decreased uric acid serum level, but did not affect plasma glucose and insulin levels. In fact, there is a trend of increasing HOMA-ir among the subjects following allopurinol administration. *In vitro*, allopurinol treatment also did not significantly change the expression of the tested mRNAs, suggesting that allopurinol's effect on diabetes control has other, complex mediative pathways. The limitations of the current study include the small size of the clinical sample and target genes.

**Conclusion:** Allopurinol administration and its related uric acid plasma reduction does not significantly affect insulin resistance; a trend however exists that allopurinol and uric acid reduction increased HOMA-ir. At the molecular level, mRNA expression of *GLUT1*, *GLUT4*, *IR-A*, and *TXNIP* is not significantly affected by allopurinol.

**Keywords:** allopurinol; diabetes mellitus; insulin resistance; hyperuricemia; *Glut4*

**Permalink/ DOI:** <https://doi.org/10.14710/jbtr.v10i3.22185>

### INTRODUCTION

Diabetes mellitus type 2 (DMT2) has been a critical and pervasive health issue globally, exerting a significant burden on individuals, healthcare systems, and societies. In Indonesia, DMT2 is also a significant health concern with a growing prevalence and substantial impact on the population's health and

economy. The country has experienced a rise in diabetes cases, with an estimated national prevalence of 10.8% in 2018, placing it among the top 10 countries with the highest prevalence of DMT2.<sup>1,2</sup>

Corresponding author:

E-mail: [alva.supit@unima.ac.id](mailto:alva.supit@unima.ac.id)  
(Alva Supit)

The 2018 nationwide Basic Health Research in Indonesia also reported a varying prevalence of DMT2 based on regions, with North Sulawesi province ranking first on the national highest proportion of obesity and hypertension, and fourth on the diabetes mellitus prevalence, thus reflecting a possible hereditary and environmental effect on DMT2 pathogenesis.<sup>1</sup> Minahasa is a majority tribe in North Sulawesi, with a reported high prevalence of DMT2 and hyperuricemia, partially attributed to their eating habit.<sup>3,4</sup> Their eating habits include high-calorie, high-fat, and high-purine diets, especially during the feasting seasons.<sup>5,6</sup> This population may reflect a unique group of people where researchers can control a single parameter (e.g. uric acid level) while keeping other parameters wild type.

Allopurinol is the first line xanthine oxidase inhibitor used in the management of hyperuricemia and its clinical manifestations, such as gout and kidney stones. This xanthine oxidase inhibition decreases the conversion of hypoxanthine to xanthine and to uric acid.<sup>7</sup> Allopurinol is rapidly absorbed after oral administration, with peak plasma concentrations occurring within 1 to 2 hours.<sup>8</sup> The drug has a bioavailability of approximately 78%, and it is only minimally bound to plasma proteins, allowing it to be widely distributed throughout the body.<sup>8</sup> Once absorbed, allopurinol is metabolized in the liver to oxypurinol, its primary active metabolite, which also inhibits xanthine oxidase.<sup>9</sup> Oxypurinol has a much longer half-life (approximately 18 to 30 hours) compared to allopurinol (1 to 2 hours), which contributes significantly to the drug's therapeutic effects. Allopurinol is excreted primarily through the kidneys, with about 80% of the dose appearing in the urine as oxypurinol and other metabolites, while the remainder is excreted unchanged. Allopurinol and oxypurinol bind to the active site of the xanthine oxidase, thus preventing the substrate from binding.<sup>10</sup> This mode of action not only decreases uric acid production but also leads to an increase in the concentration of the more soluble xanthine and hypoxanthine, which are more easily excreted.

In addition to its wide use in hyperuricemia management, allopurinol has also been studied for its potential effect on glucose levels in patients with diabetes. Several association studies have found a positive association between elevated serum uric acid levels and diabetes,<sup>11,12</sup> while others,<sup>13,14</sup> have reported an inverse relationship between increasing serum uric acid levels and diabetes mellitus. Other retrospective studies reported no correlation between UA and DMT2.<sup>15</sup> Finally, a meta-analysis by Chen et al of randomized controlled trials (RCTs) found that allopurinol use was associated with a significant reduction in fasting blood glucose (FBG) levels in the subgroup of patients without diabetes, but not in those with diabetes.<sup>16</sup> This variability demands population-specific studies to examine the allopurinol-uric acid-DMT2 relationship within each subgroup of people.

Since the previous research yielded conflicting results, the direction of correlation was an open-ended question and need to be addressed separately in different population. Therefore, in this research, we aim to study whether allopurinol administration in healthy, nondiabetic male subjects in Minahasa may lead to the

modification of HOMA-ir. Furthermore, using transcriptomic research, we also aimed to elucidate its molecular mechanism, at least partially.

## MATERIALS AND METHODS

### *Clinical study*

The clinical part of this study employed a pre- and post-test pseudo-experimental research design, where the parameters of before and after treatments were compared. The patients were conveniently drawn from the community, consisting of 22 subjects with inclusion criteria as follow: male, non-diabetic, age ranged from 20-39 years, and from the Minahasa tribe. DMT2 diagnosis for exclusion was made based on the national criteria (blood glucose >126 mg/dl after a minimum of 8 hours fasting). Five patients were excluded due to uncountable HOMA-ir. Patients received a daily dose of 300 mg allopurinol, to be taken in the morning with food for the next 3 months. Fasting blood glucose (FBG), plasma insulin (Ins) and other demographic characteristics were recorded. HOMA-ir, the parameter for insulin resistance, was calculated based on the Oxford HOMA calculator (<https://www.rdm.ox.ac.uk/about/our-clinical-facilities-and-units/DTU/software/homa>). The final parameters consisted of plasma UA level, FBG, Ins, HOMA-ir, HOMA-s (insulin sensitivity), and HOMA-b (beta cell function). Two-tailed, paired t-tests were used to calculate significant differences between pre- and post-treatment, with a significance level set to <0.05. An ethical clearance was obtained for the study (003/FIK).

### *Laboratory study*

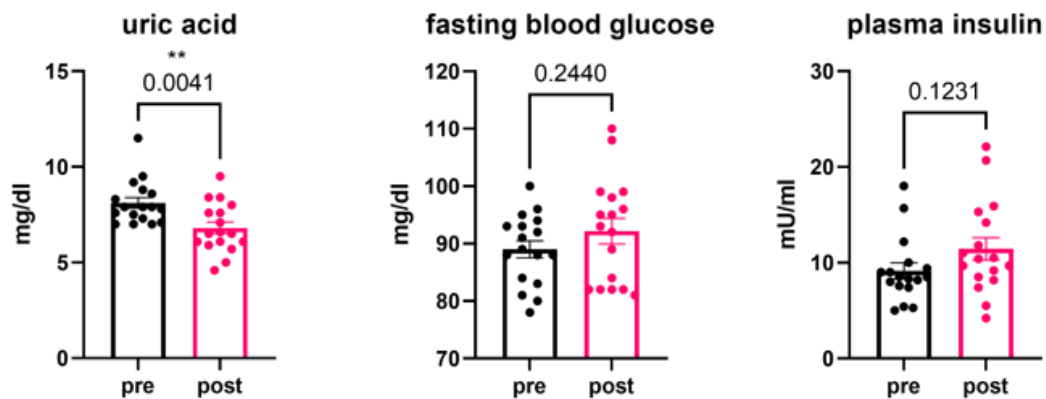
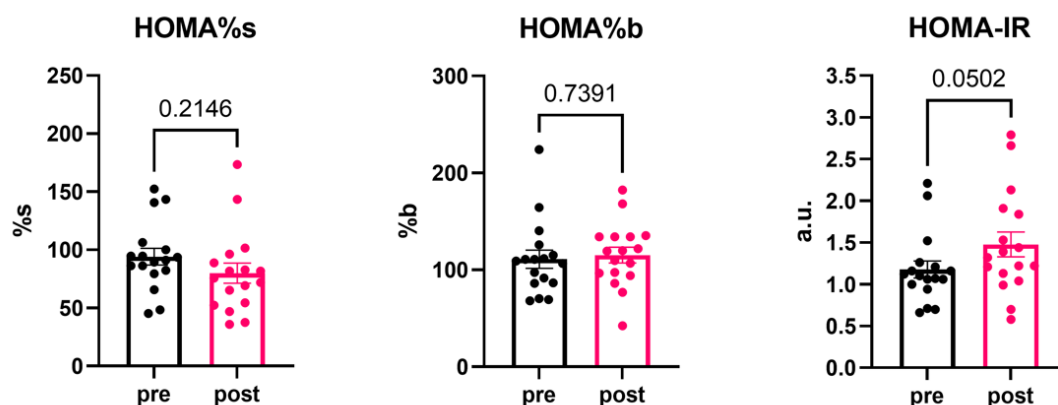
Human embryonic kidney cell line HEK293T were cultured in standard Dulbecco's Modified Eagle Medium (DMEM) with fetal bovine serum and pen/strep antibiotics in a humidified 37-degree Celsius incubator with 5% CO<sub>2</sub>. This cell line was selected because it has been well characterized in the context of glucose metabolism study and can express key protein in response to experimental treatments.<sup>17,18</sup> A low passage (p20-30) cell generations were used for the experiment. At 70% confluency, HEK293T cells were trypsin-dissociated and seeded into 6-well culture plates in DMEM and pen/strep. After 48 hours (~40% confluency), 1 or 4 mM of allopurinol were added into the cultures and incubated for another 24 hours. Another set of wells was left untreated as the control group. Experiments were done in triplicates. Cells from each well were harvested and lysed in 1 ml Trizol for further RNA extraction using the phenol-chloroform method. The resulting RNA pellets were resuspended and diluted in RNase-free ddH<sub>2</sub>O. A reverse transcriptase kit (Takara, Japan) was used to convert mRNA into cDNA. Ten nanograms of cDNA from each sample were used as a template for quantitative real-time polymerase chain reaction (qPCR). The target genes were *GLUT1* (*SLC2A1*) and *GLUT4* (*SLC2A4*) glucose transporters, glucose-dependent protein thioredoxin-interacting protein (*TXNIP*), insulin receptor subunit alpha (*IR-A*), and beta-actin (*ACTB*), a housekeeping gene for internal control. Primer pairs for these genes are presented in Table 1

**Table 1.** The primer pairs for the qPCR experiments

Gene	Forward primer sequence (5' to 3')	Reverse primer sequence (5' to 3')
<i>GLUT1</i>	CTGCTCATCAACCGCAAC	CTTCTTCTCCCGCATCATCT
<i>GLUT4</i>	TGGGCTTCTTCATCTTCACC	GTGCTGGGTTTCACCTCCT
<i>IR-A</i>	TTTTCGTCCCCAGGCCATC	GTCACATTCCCAACATCGCC
<i>TXNIP</i>	GGTCTTTAACGACCCTGAAAAGG	ACACGAGTAACCTTCACACACCT
<i>ACTB</i>	AGCCATGTACGTTGCTATCCA	ACCGGAGTCCATCACGATG

**Table 2.** Respondent characteristics

Parameter	Mean $\pm$ SD	Min value	Max value
Age (year)	30 $\pm$ 3.52	20	38
BMI (kg/m <sup>2</sup> )	27.83 $\pm$ 3.05	21.5	34.8
UA (mg/dl), pre-treatment	8.11 $\pm$ 1.16	7	11,5
UA (mg/dl), post-treatment	6.81 $\pm$ 1.30	4,6	9,5
FBG (mg/dl), pre-treatment	89.00 $\pm$ 5.15	78	100
FBG (mg/dl), post-treatment	92.18 $\pm$ 9.16	72	110
Ins (mU/mL), pre-treatment	9.15 $\pm$ 3.42	2,3	18
Ins (mU/mL), post-treatment	11.42 $\pm$ 4.86	2,3	22,1

**Figure 1.** The effect of allopurinol on uric acid, fasting blood glucose, and plasma insulin level; *pre*: before allopurinol treatment; *post*: after allopurinol treatment. Error bars are SEMs.**Figure 2.** The effect of allopurinol in HOMA-ir parameters showed no difference in insulin resistance before and after allopurinol treatment. A trend of HOMA-ir increase post-treatment is shown in HOMA-ir (right panel,  $p=0.0502$ ). Error bars are SEMs.

The qPCR mixture containing the template, primer pair, and SYBRgreen Mastermix reagent (Thermo-Fisher, USA) was amplified in an RT thermocycler (Applied Biosystem, USA). Each sample was loaded onto the 96-well plates in duplicates to account for possible technical errors. The delta-delta Ct value was used to calculate the mRNA expression foldchange. A

one-way ANOVA was used to calculate statistical significance, followed by post-hoc Dunnett's test. Graphs were generated using Prism 9.0.

## RESULTS

The respondent characteristics are presented in Table 2. As expected, allopurinol treatment decreases uric acid

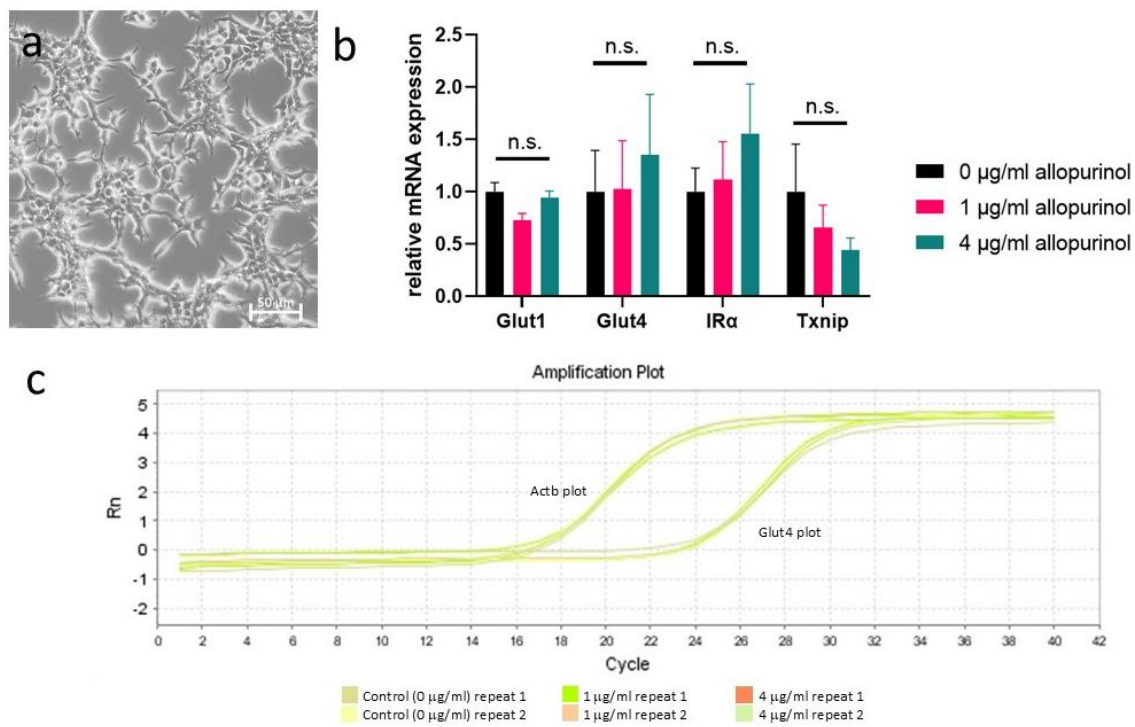


**Figure 3.** *In-vitro* analysis of allopurinol in HEK293T cell line. (a) The visual viability of the cells following 4 µg/ml allopurinol treatment; (b) the relative expression of several glucose metabolism-related mRNA (*GLUT1*, *GLUT4*, *IRα*, and *TXNIP*) under the influence of allopurinol, showing no significant, but trending differences by one-way ANOVA and post hoc Dunnet's test; (c) a representation of *GLUT4* qPCR amplification plot from one biological repeat (two technical repeats each: 0 µg/ml, 1 µg/ml and 4 µg/ml allopurinol treatment) showing overlapping plots (not significant). Error bars are SEMs, n=3 repeats.

level (average±SD pre-treatment: 8.11±1.16 mg/dl, post-treatment: 6.81±1.30 mg/dl,  $p=0.0041$ ). However, there is no difference in fasting blood glucose (pre: 89.00±5.15 mg/dl, post: 92.18±9.16 mg/dl,  $p=0.2440$ ) and plasma insulin (pre: 9.15±3.42 µU/ml, post: 11.42±4.86 µU/ml,  $p=0.1231$ , Figure 1). Following HOMA-ir calculation, we found that there is no significant difference in insulin sensitivity (HOMA%*s* pre: 94.16±29.53, post: 79.96±35.55,  $p=0.2146$ ), *b*-cell predicted function (pre: 111.06±38.52, post: 115.21±33.27,  $p=0.7391$ ), and insulin resistance (HOMA-ir pre: 1.18±0.42, post: 1.48±0.62,  $p=0.0502$ ). The statistical calculation of the latter, however, shows that there exists a trend of increasing insulin resistance following allopurinol-induced uric acid decrease (Figure 2).

We then followed up these findings with an *In vitro* experiment to further understand the possible molecular pathway involved in allopurinol-related glucose regulation. HEK293T cell line was cultured with or without allopurinol. Two concentrations (1 µg/ml and 4 µg/ml) were selected based on the *in-vivo* measurement of allopurinol and its metabolite oxypurinol.<sup>19,20</sup> There is no growth inhibition or massive cell death caused by this concentration of allopurinol *in vitro*, as can be seen from Figure 3a. Among the glucose transporter proteins, glucose transporter 4 (*GLUT4*) and glucose transporter 1 (*GLUT1*) have been well known to be crucial in glucose uptake into the cells.<sup>21</sup> Moreover, thioredoxin-interacting protein (*TXNIP*), a glucose-responsive protein, were also measured to determine the glucose uptake of the cells.<sup>22,23</sup> Insulin receptor isoform a (*IR-A*)

were also measured to see whether the glycemic effect is insulin-mediated or insulin-independent. For all these experiments, the mRNA expressions were normalized against beta-actin (*ACTB*) gene expression as the internal control. Compared to the control, both 1 and 4 µg/ml allopurinol did not significantly change the *GLUT1*, *GLUT4*, *IR-A*, and *TXNIP* expression level (Figure 3b, a representative of the qPCR amplification plot is shown in Figure 3c). However, a trend can be observed that allopurinol increases *GLUT4* and *IR-A* mRNA expression, while decreasing *TXNIP* mRNA expression, especially at the higher concentration of 4 µg/ml (Figure 3b). Altogether, these suggest that at the molecular level, allopurinol treatment may increase the *GLUT4* and insulin receptor alpha mRNA expression, which would result in an increase of glucose uptake. On the other hand, allopurinol also seems to decrease glucose uptake, as can be seen by the decreased level of *TXNIP* mRNA, which is sensitive to intracellular glucose concentration.<sup>24</sup>

## DISCUSSION

In this current research, we showed that daily administration of 300 mg allopurinol in healthy male subjects has no significant effect in insulin resistance, except for a trend of increased HOMA-ir approaching statistical significance ( $p=0.0502$ , Figure 2 right panel). Likewise, the application of 1 µg/ml allopurinol does not increase the expression of glucose transporters *GLUT1* and *GLUT4*, *IR-A*, and *TXNIP* mRNA expression *In vitro*. There are trends, however, that allopurinol increases *GLUT4* and *IR-A*, but decreases *TXNIP* mRNA expression *In vitro* when applied in supraphysiological

concentration (4 µg/ml).

The results from the current literature are already heterogeneous with conflicting results reported from different researchers. Association studies from different populations have found a positive association between elevated serum uric acid levels and diabetes,<sup>11,12</sup> while others<sup>13,14</sup> have reported that serum uric acid levels is negatively correlated with glycaemic control. Other retrospective studies reported no correlation between uric acid level and DMT2.<sup>15</sup> When analysed together, meta-analysis of randomized controlled trials (RCTs) found that allopurinol use was associated with a significant reduction in fasting blood glucose (FBG) levels in the subgroup of patients without diabetes, but not in those with diabetes.<sup>16</sup> In our samples, there exists a trend that allopurinol administration and its related uric acid lowering actually increased insulin resistance, although it did not reach statistical significance. Our population (adult, non-diabetic males from the Minahasa tribe) is unique in the way that they have a high-calorie, high-fat, and high-purine diet.<sup>3-6</sup> When allopurinol treatment was initiated, we did not give specific instructions on how to control the subjects' diet, (i.e. the subjects were told "Please eat like you usually do"). Although this may increase the confounding variables, it is superior in reflecting the conditions in the community settings. Indeed, we found that allopurinol without any other diet modification had already shown a decrease in uric acid level, which is expected to be shown by an established drug. Interestingly, as a side effect, insulin resistance seems to be increased in our samples. Due to the nature of this pseudo-experiment, it is not possible to elucidate whether this increase reflects a physiological dynamic, the natural history of an ongoing disease progression, or a direct consequence of allopurinol and uric acid lowering. Moreover, DMT2 is a multifactorial disease, with both genetic and lifestyle contributing to its pathogenesis. Therefore, in different populations, the effect of allopurinol and urate-lowering therapy may be variable, thus similar research in different population settings is mandatory to tailor a comprehensive approach to DMT2 management.

*In vivo*, allopurinol is rapidly metabolized to oxypurinol. After oral administration, allopurinol may rise to 1 µg/mL within the first several hours, before metabolized to oxypurinol.<sup>19</sup> The plasma concentration may rise to 4 µg/mL when administered intravenously in experimental setting.<sup>16</sup> We chose these as the working concentrations. At both 1 µg/ml and 4 µg/ml, the growth of HEK293T cells was not affected by allopurinol, suggesting the nontoxicity of the treatment. A trend of change can be observed in *GLUT4*, *IR-A*, and *TXNIP* expression over increasing allopurinol concentration, but they did not reach statistical significance. The results from our experiment may be explained by several things. First, allopurinol shows a weaker xanthine oxidoreductase inhibition compared to its metabolite, oxypurinol,<sup>10</sup> while *In vivo*, allopurinol is rapidly metabolized to oxypurinol. This pharmacokinetic response could not be replicated *In vitro*, thus, an *In vivo* experimental study in animal models is needed. Results from animal studies mostly highlighted the effect of allopurinol on the complications of diabetes. For example, allopurinol decreases kidney injury in diabetic

mice,<sup>25</sup> ameliorates hepatic steatosis,<sup>26</sup> and alleviates cardiac anomaly in insulin resistance,<sup>27</sup> but does not affect insulin resistance *per se*. Whether these effects are mediated by allopurinol, oxypurinol, or due to the uric acid lowering is not fully understood.

Although both our clinical and molecular studies did not reach statistical significance, interesting trends emerged from these current results. Allopurinol seems to increase insulin resistance in healthy, nondiabetic male subjects. At the molecular level, the expressions of *IR-A* and *GLUT4* also tend to increase, suggesting that the glucose uptake should actually increase, resulting in less insulin resistance. However, the expression of *TXNIP* also tends to increase, thus suggesting a failure in uptaking the glucose from the culture medium.<sup>24</sup> Together, these results suggest that the effect of allopurinol on the expression of key protein related in glucose metabolism is versatile, depending not only on the cellular context *in vitro*,<sup>28</sup> but also on the physiological condition at the organismal level,<sup>29</sup> e.g. one gene may be expressed differentially in different individuals as a response to allopurinol. This complex molecular response can also explain the heterogeneity in the results of previous clinical research results<sup>11-16</sup> in determining whether allopurinol increase or decrease insulin resistance.

Further research is necessary to fully capture the complex molecular mechanism of DMT2 and insulin resistance at the molecular levels. For example, controlling the dietary intake of the clinical experiment subjects for the duration of allopurinol administration is a way to control for confounding factors. More samples from more heterogeneous populations and longer follow-up duration will also increase the power of future studies. In terms of molecular studies, including more genes involved in DMT2 pathogenesis will also provide a clearer explanation about the effect of allopurinol in DMT2. These include glucagon receptors, other subunit of insulin receptors, IL1, glucocorticoid receptor, among others.

## CONCLUSION

The administration of allopurinol 300 mg daily for three months without any diet modification does not have a significant effect on insulin resistance. However, a trend existed indicating that allopurinol administration and uric acid lowering increase insulin resistance, which may be explained by the complex interaction between allopurinol and glucose metabolism-related genes. Further research involving larger clinical subjects and more molecular pathways is necessary to fully understand the mechanism of uric acid-related glycemic control.

## REFERENCES

1. Indonesian Ministry of Health. Riset Kesehatan Dasar. Published online 2018. Accessed February 19, 2024. [https://kesmas.kemkes.go.id/assets/upload/dir\\_519d41d8cd98f00/files/Hasil-risikesdas-2018\\_1274.pdf](https://kesmas.kemkes.go.id/assets/upload/dir_519d41d8cd98f00/files/Hasil-risikesdas-2018_1274.pdf)

2. Soeatmadji DW, Rosandi R, Saraswati MR, Sibarani RP, Tarigan WO. Clinicodemographic Profile and Outcomes of Type 2 Diabetes Mellitus in the Indonesian Cohort of DISCOVER: A 3-Year Prospective Cohort Study. *J ASEAN Fed Endocr Soc.* 2023;38(1):68. doi:10.15605/jafes.038.01.10
3. Reagen M. The Relationship Between Eating Wild Animal Meat with the Level of Uric Acid in Langowan Minahasa, Indonesia. *KnE Life Sci.* Published online 2019:511066. doi:10.18502/cls.v4i13.5226
4. Supit A, Telew A, Bawiling N. The Church, Food Culture, and Ecotheology: An Ongoing Church Effort to Reduce Bushmeat Eating in Minahasa, Indonesia. *Christ J Glob Health.* 2021;8(1):64-68. doi:10.15566/cjgh.v8i1.537
5. Kandou GD. The Influence of Eating Habits Of Minahasan Dishes On The Occurrence Of Coronary Heart Disease. *J BiomedikJBM.* 2010;2(3) doi:10.35790/jbm.2.3.2010.1196
6. Weichart G. Makan dan minum bersama: feasting commensality in Minahasa, Indonesia. *Anthropol Food.* 2008;(S3). doi:10.4000/aof.2212
7. Wen J, Chen S, Deng L, et al. Inhibitory mechanism of phloretin on xanthine oxidase and its synergistic effect with allopurinol and febuxostat. *Food Biosci.* 2024;61:104720.
8. Al-Dalaen SM, Hamad AWR, Al-Saraireh F, Alkaraki RN, Magarbeh MKM, Abid FM. Bioavailability and bioequivalence of allopurinol in two tablet formulations. *Biomed Pharmacol J.* 2020;13(2):789-798.
9. Chu WY, Annink KV, Nijstad AL, et al. Pharmacokinetic/pharmacodynamic modelling of allopurinol, its active metabolite oxypurinol, and biomarkers hypoxanthine, xanthine and uric acid in hypoxic-ischemic encephalopathy neonates. *Clin Pharmacokinet.* Published online 2022:1-13. doi: 10.1007/s40262-021-01068-0
10. Sekine M, Okamoto K, Pai EF, et al. Allopurinol and oxypurinol differ in their strength and mechanisms of inhibition of xanthine oxidoreductase. *J Biol Chem.* 2023;299(9):105189. doi:10.1016/j.jbc.2023.105189
11. Alqahtani SAM, Awan ZA, Alasmary MY, Al Amoudi SM. Association between serum uric acid with diabetes and other biochemical markers. *J Fam Med Prim Care.* 2022;11(4):1401-1409. doi:10.4103/jfmpc.jfmpc\_1833\_21
12. IAnothaisintawee T, Lertrattananon D, Thamakaisan S, Reutrakul S, Ongphiphadhanakul B, Thakkestian A. Direct and Indirect Effects of Serum Uric Acid on Blood Sugar Levels in Patients with Prediabetes: A Mediation Analysis. *J Diabetes Res.* 2017;2017:e6830671. doi:10.1155/2017/6830671
13. Bandaru P, Shankar A. Association between Serum Uric Acid Levels and Diabetes Mellitus. *Int J Endocrinol.* 2011;2011:604715. doi:10.1155/2011/604715
14. Haque T, Rahman S, Islam S, Molla NH, Ali N. Assessment of the relationship between serum uric acid and glucose levels in healthy, prediabetic and diabetic individuals. *Diabetol Metab Syndr.* 2019;11(1):49. doi:10.1186/s13098-019-0446-6
15. Slobodnick A, Toprover M, Greenberg J, et al. Allopurinol use and type 2 diabetes incidence among patients with gout: A VA retrospective cohort study. *Medicine (Baltimore).* 2020;99(35):e21675. doi:10.1097/MD.00000000000021675
16. Chen J, Ge J, Zha M, Miao JJ, Sun ZL, Yu JY. Effects of Uric Acid-Lowering Treatment on Glycemia: A Systematic Review and Meta-Analysis. *Front Endocrinol.* 2020;11. doi: 10.3389/fendo.2020.00577
17. Wang Y zhe, Yang D hua, Wang M wei. Signaling profiles in HEK 293T cells co-expressing GLP-1 and GIP receptors. *Acta Pharmacol Sin.* 2022;43(6):1453-1460. doi:10.1038/s41401-021-00758-6
18. Stepanenko AA, Dmitrenko VV. HEK293 in cell biology and cancer research: phenotype, karyotype, tumorigenicity, and stress-induced genome-phenotype evolution. *Gene.* 2015;569(2):182-190. doi:10.1016/j.gene.2015.05.065
19. Turnheim K, Krivanek P, Oberbauer R. Pharmacokinetics and pharmacodynamics of allopurinol in elderly and young subjects. *Br J Clin Pharmacol.* 1999;48(4):501-509. doi:10.1046/j.1365-2125.1999.00041.x
20. Liu X, Ni XJ, Shang DW, et al. Determination of allopurinol and oxypurinol in human plasma and urine by liquid chromatography-tandem mass spectrometry. *J Chromatogr B.* 2013;941:10-16. doi:10.1016/j.jchromb.2013.09.028
21. Arponen M, Jalava N, Widjaja N, Ivaska KK. Glucose transporters GLUT1, GLUT3, and GLUT4 have different effects on osteoblast proliferation and metabolism. *Front Physiol.* 2022;13:1035516. doi: 10.3389/fphys.2022.1035516
22. Parikh H, Carlsson E, Chutkow WA, et al. TXNIP regulates peripheral glucose metabolism in humans. *PLoS Med.* 2007;4(5):e158. doi: 10.1371/journal.pmed.0040158
23. Yoshihara E. TXNIP/TBP-2: a master regulator for glucose homeostasis. *Antioxidants.* 2020;9(8):765. doi: 10.3390/antiox9080765
24. Choi EH, Park SJ. TXNIP: A key protein in the cellular stress response pathway and a potential therapeutic target. *Exp Mol Med.* 2023;55(7):1348-1356. doi: 10.1038/s12276-023-01019-8
25. Kosugi T, Nakayama T, Heinig M, et al. Effect of lowering uric acid on renal disease in the type 2 diabetic db/db mice. *Am J Physiol-Ren Physiol.* 2009;297(2):F481-F488. doi:10.1152/ajprenal.00092.2009
26. Cho IJ, Oh DH, Yoo J, et al. Allopurinol ameliorates high fructose diet induced hepatic steatosis in diabetic rats through modulation of lipid metabolism, inflammation, and ER stress pathway. *Sci Rep.* 2021;11(1):9894. doi:10.1038/s41598-021-88872-7

- 
27. El-Bassossy HM, Watson ML. Xanthine oxidase inhibition alleviates the cardiac complications of insulin resistance: effect on low grade inflammation and the angiotensin system. *J Transl Med.* 2015;13(1):82. doi:10.1186/s12967-015-0445-9
  28. Henquin JC. Glucose-induced insulin secretion in isolated human islets: Does it truly reflect  $\beta$ -cell function *In vivo*? *Mol Metab.* 2021;48:101212. doi: 10.1016/j.molmet.2021.101212
  29. Wachsmuth HR, Weninger SN, Duca FA. Role of the gut–brain axis in energy and glucose metabolism. *Exp Mol Med.* 2022;54(4):377-392. doi: 10.1038/s12276-021-00677-w
-



# JOURNAL OF BIOMEDICINE AND TRANSLATIONAL RESEARCH

Available online at JBTR website: <https://jbtr.fk.undip.ac.id>

Copyright©2024 by Faculty of Medicine Universitas Diponegoro, Indonesian Society of Human Genetics and Indonesian Society of Internal Medicine

Original Research Article

## Effects of Coal Dust Exposure in Eosinophil and Interleukin (IL)-13 on Pulmonary Remodeling in Asthmatic Mice Models

Fujiati Fujiati<sup>1</sup>, Haryati Haryati<sup>2\*</sup>

<sup>1</sup>Department of Biochemistry and Biomolecular, Faculty of Medicine, Universitas Lambung Mangkurat, Indonesia

<sup>2</sup>Department of Pulmonology and Respiratory Medicine, Faculty of Medicine, Universitas Lambung Mangkurat, Indonesia

### Article Info

History

Received: 12 Mar 2024

Accepted: 12 Nov 2024

Available: 30 Dec 2024

### Abstract

**Background:** Coal dust is a source of pollution that increases the likelihood of respiratory diseases, including asthma. The combination of asthma and coal dust pollution is associated with inflammation cell activation and pulmonary remodeling. Eosinophils and Interleukin (IL)-13 as inflammatory cells and cytokines also play a role in asthma's pathogenesis and development. This study investigates the impact of coal dust exposure on eosinophil and IL-13 levels in an asthmatic mice-like model on pulmonary remodeling.

**Methods:** An experiment was conducted on 20-25 g BALB/c mice aged 6 to 12 weeks. The three groups had ten mice each. Groups were sensitized with normal saline, ovalbumin (OVA)-sensitized, and OVA-sensitized + coal dust. The parameters of pulmonary remodeling (the thickness of the epithelium, smooth muscle thickness, the number of goblet cells, and subepithelial fibrosis) and the number of eosinophils were measured with histomorphometry analysis. Total IL-13 concentrations were measured using an IL-13 ELISA kit. The data group of a combination of OVA + coal dust was analyzed using the path analysis method.

**Results:** From path analysis, it was found that Eosinophils ( $b=0.006$ ; 95%CI=-2.594 to 2.606;  $p=0.000$ ) had positive, direct, and statistically significant effects on IL-13. Eosinophils indirectly affected epithelium thickness and subepithelial fibrosis thickness via IL-13. Interleukine-13 had positive, direct, and statistically significant effects on epithelium thickness ( $b=0.67$ ; 95%CI=-0.129 to 1.471;  $p=0.010$ ) and subepithelial fibrosis thickness ( $b=0.682$ ; 95%CI=0.301 to 1.062;  $p=0.000$ ).

**Conclusion:** Eosinophils' indirect effect on pulmonary remodeling via IL-13 and IL-13 directly affects airway remodeling, especially epithelium and subepithelial fibrosis components.

**Keywords:** Airway remodeling; Asthma, Coal dust; Eosinophil; IL-13

**Permalink/ DOI:** <https://doi.org/10.14710/jbtr.v10i3.22243>

### INTRODUCTION

Pulmonary remodeling is a cellular and tissue structure transformation caused by the intrusion of foreign substances into the lungs, such as allergens, air pollutants, and others. Asthmatic individuals display airway remodeling. Characterizations of airway remodeling in asthma include epithelial thickness, smooth muscle hypertrophy, goblet cell hyperplasia, and subepithelial fibrosis.<sup>1,2</sup> Changes in pulmonary structure affect mechanical features such as decreased lung compliance, airflow limits, reduced pulmonary function,

and increased airway hyper-reactivity compared to persons without health issues.<sup>3</sup>

Pulmonary remodeling in asthma involves many inflammatory mediators. In asthma, eosinophilic and cytokine dominant inflammation from T-helper2/Th2 lymphocytes such as IL-4, IL-5, IL-9, and IL-13.

\*Corresponding author:

E-mail: [haryati@ulm.ac.id](mailto:haryati@ulm.ac.id)

(Haryati Haryati)



Mediators such as histamine, leukotrienes, prostaglandins, and cytokines can cause bronchial spasm, edema, increased mucus secretion, and bronchial smooth muscle contractions in asthma.<sup>3</sup> Eosinophils increase the secretion of proteolytic enzymes, growth factors (transforming growth factor/TGF- $\beta$ , platelet-derived growth factor/PDGF, fibroblast growth factor/FGF), and oxidative products involved in pulmonary remodeling. Interleukin-13 triggers collagen production and proliferation in fibroblasts and activates TGF- $\beta$  by upregulating matrix metalloproteinase/MMP.<sup>4</sup> T cells, mast cells, basophils, dendritic cells, and keratinocytes are a few examples of immune and nonimmune cells identified as IL-13 producers. According to some theories, IL-13 acts as an activator, chemotactic, and survival factor for eosinophils. Part of the way that IL-13 encourages eosinophilic inflammation is by increasing the expression of chemokines that attract eosinophils and bind to CCR3.

IL-13 promotes leucocytes and resident airway cells to produce CCR4-binding chemokines, which are more prevalent in allergic asthma patients.<sup>5</sup>

Air pollution causes decreased airway function in asthmatic patients.<sup>6</sup> Other studies have reported a relationship between asthmatic exacerbation and air pollution containing PM 2.5, ozone (O<sub>3</sub>), and nitrate dioxide (NO<sub>2</sub>).<sup>7</sup> Coal dust is one of the air pollutants containing various organic and inorganic compounds that could trigger inflammation and changes in lung structure, like pulmonary remodeling. Repeated exposure to the airway has been documented to induce harmful respiratory consequences, including asthma.<sup>8</sup> The pathogenesis of the progression of pulmonary remodeling is thought to involve the release of cytokines, chemokines, and growth factors from both inflammatory cells and structural cells due to the induction of exogenous agents. Acute exposure to coal dust induces a pulmonary immune response by increasing the

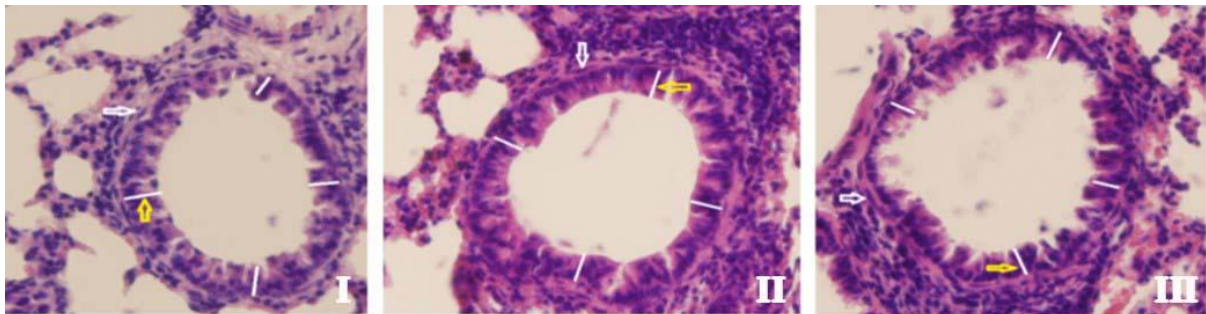


**Figure 1.** The HE staining of the mouse bronchioles' epithelial histology and smooth muscle (scale 100  $\mu$ m, 400x magnification); the yellow arrow denotes epithelial thickness. The white arrow indicates smooth muscle. I = Control, II = OVA, and III = OVA + coal dust.

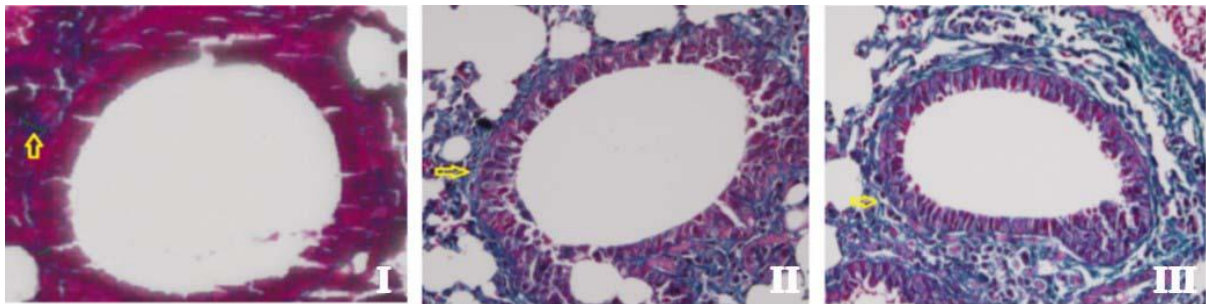


**Figure 2.** Masson's Trichrome staining of fibrosis subepithelial bronchioles in mice (scale 100  $\mu$ m, 400x magnification). The yellow arrow indicates the thickness of subepithelial fibrosis. I = Control, II = OVA, and III = OVA + coal dust.

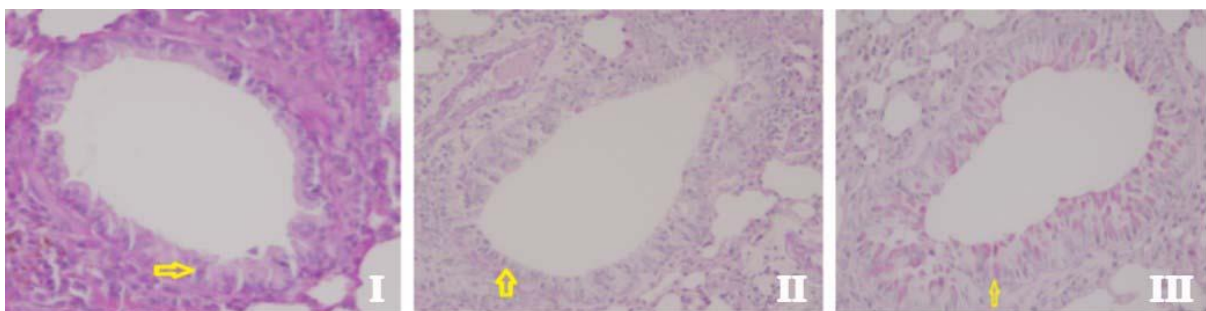


**Figure 3.** Image of mouse bronchioles goblet cells stained with PAS (scale 100  $\mu$ m, 400x magnification). The yellow arrow indicates the goblet cell. I=Control; II=OVA; III= OVA + coal dust.

infiltration of leukocytes, neutrophils, and alveolar macrophages.<sup>9,10</sup> In the serum of coal mine workers was found an increase in IL-1 $\beta$ , TNF- $\alpha$ , and IL-6.<sup>11</sup>

Nonetheless, despite the clinical significance of airway remodeling, the mechanism behind its induction to airway epithelial cells, inflammatory cells, and cytokines remains unclear, with only limited studies investigating this topic. An animal model treated with ovalbumin helps research airway remodeling, and subjecting the model to repeated chronic exposure to allergens could lead to chronic inflammation and subsequent airway remodeling. Therefore, this study investigates the pulmonary remodeling process in asthmatic mice exposed to coal dust over a prolonged period. We examined the changes in inflammatory cells such as eosinophil and cytokine (IL-13) in bronchoalveolar lavage and how they impact pulmonary remodeling after exposure to coal dust in animal models of asthma.

## MATERIALS AND METHODS

### Animal model

Thirty *Mus musculus* (BALB/c), mice from the Farma Veterinary Center in Surabaya, consisting of only females, as they respond better to allergens than males.<sup>12</sup> The inclusion criteria were mice aged 6-12 weeks weighing 20-25 g with a health condition and disease-free (good food consumption, good activity, and no hair loss). All test animals were acclimatized for seven days in the Biochemistry and Biomolecular Laboratory of the Faculty of Medicine, Universitas Lambung Mangkurat. The experimental animals were provided with food and water according to laboratory standards. Experimental animals were divided randomly into three treatment groups, each consisting of 10 mice: (I) negative control; (II) 1% OVA sensitization; (III) OVA 1% sensitization and exposure to coal dust size  $\leq 5\mu\text{m}$  concentration of 12.5 mg/m<sup>3</sup>. Twenty-four hours after the last exposure on day 76, the mice were killed by anesthetized intraperitoneally with ketamine at 150 mg/kg BW and midazolam at 0.5 mg/kg BW. Then, surgery is performed to take bronchoalveolar lavage fluid. An intravenous catheter is inserted through an incision in the trachea, and then the lungs are rinsed with cold saline. The rinse results for eosinophil and IL-13 examination. The lung organ is taken for histomorphometry examination. The ethics committee Faculty of Medicine, Universitas Lambung Mangkurat approved this research with No. 304/KEPK-FK UNLAM/EC/IV/2017).

### Ovalbumin (OVA) sensitization

The negative controls received an intraperitoneal (i.p) injection of 1 mg Al(OH)<sub>3</sub> in 0.5 ml of normal saline and inhalation of normal saline. The remaining two groups were sensitized and exposed to ovalbumin (OVA) and coal dust. The allergen used was chicken ovalbumin (TCI®). The initial sensitization was performed by administering intraperitoneal injections (i.p) of 10g OVA and 1 mg Al(OH)<sub>3</sub> in 0.5 ml normal saline on days 0 and 14. Furthermore, the repeat sensitization involved inhaling OVA 1% using a nebulizer of type NU-017 for 20 minutes, three times per week, for 8 weeks. This process starts from day 21-75.<sup>13</sup>

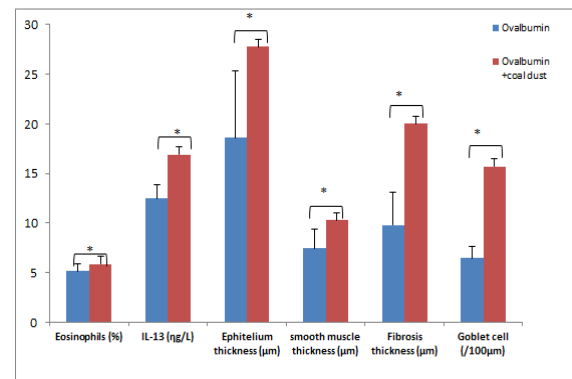


**Figure 4.** Comparison graph of the number of eosinophils and levels of IL-13 pulmonary remodeling between OVA group with a combination of OVA+coal dust group. Values are presented in mean  $\pm$  SD. \* $p$  < 0.05, statistically t-independent test significant.

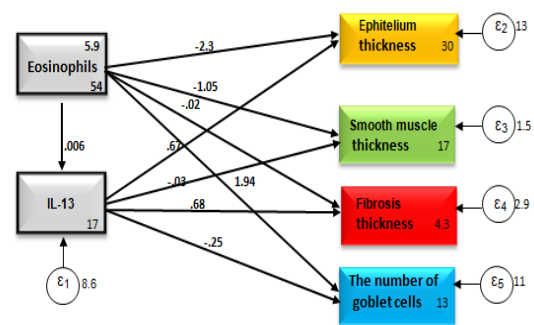


**Figure 5:** Identification of the path analysis model.

### Coal dust creation and exposure

A total of 2 kg of coal were crushed with a pulverizing tool. Making coal dust was conducted in the Carsurin Coal Banjarmasin laboratory. The particles produced were then filtered using a 5  $\mu\text{m}$  PVC chiffon filter to obtain coal dust size  $\leq 5\mu\text{m}$ .<sup>10</sup>

The exposure to coal dust after four weeks of OVA sensitization. It used a chamber size of 30x30x30 cm<sup>3</sup> with 1.5–2 L/min airflow that resembled the environmental coal mine airflow available at the Biochemistry and Biomolecular Laboratory, Faculty of Medicine, Universitas Lambung Mangkurat. This tool provides an ambient environment containing coal dust exposure to the animal's airway for 1 hour/day for four weeks on days 45-75. An oxygen supply is also provided in the chamber to prevent hypoxia and discomfort. The negative control group was only exposed to room air.<sup>10</sup>

### The IL-13 measurement concentrations from lung-homogenate supernatant

Tissues from the left lung were sonicated and mechanically homogenized in a 50 mM Tris-HCl buffered solution at a pH of 7.4. At 40 degrees Celsius, the homogenate was centrifuged at 3200 rpm for two minutes. The lung homogenate supernatant was utilized for the IL-13 determination.<sup>10</sup> Per the manufacturer's instructions, the lung homogenate supernatant was quantified using ELISA kits (Bioassay Technology laboratory/Cat.No. E0019Mo). The Central Biomedical Laboratory, Faculty of Medicine, Universitas Brawijaya, analyzed IL-13.<sup>10</sup>

**Table 1.** Comparison of the number of eosinophils and levels of IL-13 pulmonary remodeling between the OVA group with a combination of OVA + coal dust group.

Variable (mean $\pm$ SD)	OVA	OVA + Coal Dust	<i>p</i> -value
Eosinophils (%)	5.167 $\pm$ 0.75	5.889 $\pm$ 0.782	<b>0.014</b>
IL-13 (ng/L)	12.494 $\pm$ 1.382	16.927 $\pm$ 3.111	<b>0.005</b>
Epithelium thickness ( $\mu$ m)	18.607 $\pm$ 6.727	27.763 $\pm$ 4.709	<b>0.005</b>
Smooth muscle thickness ( $\mu$ m)	7.444 $\pm$ 1.925	10.290 $\pm$ 1.549	<b>0.005</b>
Fibrosis thickness ( $\mu$ m)	9.79 $\pm$ 3.293	20.018 $\pm$ 3.843	<b>0.000</b>
Goblet cell (/100 $\mu$ m)	6.444 $\pm$ 1.255/10	15,692 $\pm$ 2,790/100	<b>0.000</b>

**Table 2.** Results of the analysis of the factor pathways that affect pulmonary remodeling using the eosinophil and IL-13 pulmonary tissue approach

Variable dependent	Variable independent	Coef. Std. Err	95% Conf. Interval		<i>p</i>
Direct effects					
Epithelium thickness	←Eosinophils	-2.335	-5.518	0.847	0.150
	←IL-13	0.671	-0.129	1.471	<b>0.010</b>
Smooth muscle thickness	←Eosinophils	-1.048	-2.144	0.047	0.061
	←IL-13	-0.032	-0.308	0.243	0.818
Fibrosis thickness	←Eosinophils	-0.017	-1.532	1.498	0.983
	←IL-13	0.682	0.301	1.062	<b>0.000</b>
Goblet cells	←Eosinophils	1.938	-0.942	4.818	0.187
	←IL-13	-0.249	-0.973	0.474	0.499
Indirect effects					
Epithelium thickness, Fibrosis thickness	← IL-13 ← Eosinophils	0.006	-2.594	2.606	<b>0.000</b>

Log like hood= -112.398; N observation=9; df=19; AIC=262.795; BIC=266.542 (path analysis method STATA MP13)

### Eosinophil's lung-homogenate supernatant analysis

The supernatant was obtained from the left lung homogenate for eosinophil examination. One drop of supernatant was placed on the slide, fixed, and stained using Wright-Giemsa stain. One hundred cells were examined on each slide using established criteria to categorize different types of white blood cells. The analysis of eosinophils in the Central Biomedical Laboratory, Faculty of Medicine, Universitas Brawijaya.

### Histomorphometry analysis

The histological study was analyzed in the Pathology Anatomy Laboratory, Faculty of Medicine, Universitas Brawijaya. The right lung was preserved with 10% formalin, blocked with paraffin, and microtome to a thickness of 3 mm. Hematoxylin-eosin (HE) staining was utilized to determine the epithelium's and smooth muscle's thickness. The periodic acid Schiff (PAS) technique measured the goblet cell. In contrast, bronchioles subepithelial fibrosis was measured with Massch's Trichome staining collagen deposition by examining blue-stained positive spots chosen beneath the basement membrane. The slides were examined using an Olympus BX51 light microscope at magnifications of 100x and 400x. Three fields of view were observed on each preparation. The photographs were taken with an Olympus DP71 digital camera. Morphometric investigation of structural modifications utilizing Image-Pro Plus 6.1 (Media Cybernetics, Silver Spring, MD).

### Statistical analysis

The differentiation between the number of eosinophils and IL-13 level with histomorphometry parameters (epithelial thickness, smooth muscle

thickness, subepithelial fibrosis thickness, and bronchial goblet cells) between the two treatment groups (OVA vs OVA + coal dust) was carried out through an independent t-test. STATA/MP 13 (StataCorp LP, College Station, TX, USA) was used to investigate the impact of eosinophil count and IL-13 levels on histomorphometry parameters. The results are presented as the mean  $\pm$  standard deviation (SD) and  $\beta$  coefficient, with statistical significance at  $p < 0.05$ .

### RESULTS

This study revealed that combining OVA and coal dust increased the number of eosinophils, IL-13 levels, epithelial thickness, smooth muscle thickness, subepithelial fibrosis thickness, and bronchial goblet cells compared to OVA alone (Figure 1-3). The epithelial thickness, smooth muscle thickness, subepithelial fibrosis thickness, and bronchial goblet cells numbers of the ovalbumin epithelium + coal dust were significantly higher than the ovalbumin sensitization group with (27.763  $\pm$  4.70  $\mu$ m vs. 18.607  $\pm$  6.727  $\mu$ m,  $p = 0.005$ ), (10.290  $\pm$  1.549  $\mu$ m vs. 7.444  $\pm$  1.925  $\mu$ m,  $p = 0.005$ ), (20.018  $\pm$  3.843  $\mu$ m vs. 9.79  $\pm$  3.293  $\mu$ m,  $p = 0.000$ ) and (15.692  $\pm$  2.790/100 vs. 6.444  $\pm$  1.255/100,  $p = 0.000$ ), respectively. The t-independent analysis found significant differences (Table 1 and Figure 4).

### Eosinophil

Table 1 shows that the number of eosinophils in the ovalbumin + coal dust combination group (5.889  $\pm$  0.782%) was significantly higher than in the ovalbumin sensitization group (5.167  $\pm$  0.75%) ( $p = 0.014$ ). Table 2 shows that eosinophils do not directly affect pulmonary

remodeling but indirectly via IL-13 on epithelial and subepithelial fibrosis thickness.

### IL-13 level

The levels of IL-13 ovalbumin + coal dust group ( $16.927 \pm 3.111$  ng/L) were significantly higher than the ovalbumin group ( $12.494 \pm 1.382$  ng/L) ( $p = 0.005$ ) (Table 1). Table 2 displays that IL-13 directly influences the thickness of the epithelial and subepithelial fibrosis of the bronchi and bronchioles.

The path coefficient value of each variable shown in Table 1 is more than zero and statistically significant. It shows that the model created in the path analysis in Figure 5 processing with STATA/MP 13 is based on the existing sample data. Therefore, it is unnecessary to re-validate the path analysis model.

## DISCUSSION

### Effect of eosinophils lung tissue on pulmonary remodeling after exposure to coal dust in an asthma mice model

This study showed that eosinophils do not directly affect lung remodeling. Allergic host reactions involve eosinophils. Degranulation of cationic proteins in cytoplasmic granules is linked to their effector activities. The ability of eosinophils to generate cytokines that mediate a wide range of actions in the local environment has led to the recognition of more diversified functions for eosinophils in multiple tissue areas where they were previously dismissed.<sup>14</sup>

Eosinophils from mice are a source of several cytokines. For instance, mouse eosinophils have mRNA and protein for a ligand that induces proliferation (IL-4, IL-6, IL-10, and TNF- $\alpha$ ). Mouse eosinophils produce both type 1 and many chemokines and type 2 cytokines.<sup>15-17</sup> Eosinophils produce several cytokines, such as IL-13, which triggers airway hyperresponsiveness (AHR) and promotes excessive mucus production by stimulating the growth of goblet cells. Mice that did not have eosinophils were shielded from airway hyperresponsiveness (AHR) and excessive mucus production.<sup>18</sup> The Cysteinyl leukotrienes (CysLTs) in asthma significantly exacerbate asthma. In asthmatic patients, there is a substantial association between eosinophil counts and cysteine leukotriene receptor 2 (CyLTR2 M01 V) polymorphism.<sup>19</sup> Goblet cell hyperplasia, collagen deposition,  $\alpha$ -smooth muscle actin expression, and profibrotic gene expression are signs of AHR and slow airway remodeling. They can decrease by the leukotriene receptor inhibitor treatment.<sup>20</sup>

Eosinophils secrete several growth factors and fibrogenic mediators to stimulate airway remodeling. Eosinophils are the main source of TGF- $\beta$  in the bronchial biopsies of asthmatic patients and can stimulate epithelial cells to release various mediators, including TGF- $\beta$ .<sup>21</sup> TGF- $\beta$  plays a role in modifying tissues by causing an increase in the number and size of smooth muscle cells, and it controls the activity of fibroblasts that promote fibrosis.<sup>22</sup> Following decreasing eosinophil numbers, TGF- $\beta$  mRNA expression decreases.<sup>23</sup>

### Effect of IL-13 lung tissue on bronchial and bronchiole epithelium thickness after exposure to coal dust in an asthma mice model

The results showed a significant positive effect between IL-13 lung tissue and epithelium thickness. Interleukin 13 increases the bronchial epithelium's and bronchioles' thickness had a log odd 0.67 times ( $b = 0.67$ ; 95% CI = -0.129 to 1.471;  $p = 0.010$ ). Each increase in IL-13 lung tissue will increase the thickness of the epithelium by 0.67 times. This study's results are consistent with Everman et al.'s studies that said the direct interaction of IL-13 with epithelial cells increases epithelial cell proliferation in vitro.<sup>24</sup> Other studies mentioned that IL-13R $\alpha$ 2 inhibition would inhibit IL-13 signaling, which causes decreased expression and secretion of growth factors that play a role in repair and are related to airway remodeling.<sup>25</sup>

### Effect of IL-13 lung tissue on bronchial and bronchiole smooth muscle thickness after exposure to coal dust in an asthma mice model

The results showed an insignificant influence between IL-13 lung tissue and smooth muscle thickness. Interleukin 13 had a log odd to reduce bronchial smooth muscle thickness and bronchioles -0.032 times ( $b = -0.032$ ; 95% CI = -0.308 to 0.243;  $p = 0.818$ ). The findings of this study contrast with those of another study, which stated that the basic fibroblast growth factor (bFGF) is among the factors released by IL-13 in airway smooth muscle cells, promoting smooth muscle cell proliferation.<sup>26</sup> Another review mentioned that IL-13 affects the proliferation of bronchial smooth muscle cells through increased regulation of cysteine leukotriene receptors (cysLT1R) in response to LTD4.<sup>27</sup> Understanding the causes of airway smooth muscle hyperplasia or hypertrophy, regardless of IL-13, can provide insights into how asthma mice model interact with coal dust exposure. Severe pulmonary remodeling due to coal dust exposure in an asthma mice model can trigger smooth muscle cell responses, regardless of IL-13 signals during sub-chronic exposure to coal dust. It may be the involvement of other mediators induced by coal dust, such as IL-8, eotaxin, and MIP-1 $\alpha$  reduces the rate of apoptosis of smooth muscle cells in smooth muscle cells, not asthmatics.<sup>28</sup>

### Effect of IL-13 lung tissue on bronchial and bronchiole subepithelial fibrosis thickness after exposure to coal dust in an asthma mice model

The results showed a positive and significant effect between IL-13 pulmonary tissue and increased thickness of subepithelial fibrosis after exposure to coal dust in asthma mice models. Interleukin 13 had a log odd to increase thick bronchial and subepithelial bronchial fibrosis 0.68 times ( $b = 0.682$ ; 95% CI = 0.301 to 1.062;  $p = 0.000$ ). Inflammation (via eosinophils and B cells) and remodeling (by fibroblasts, airway smooth muscle, dendritic cells, and epithelial cells) are stimulated by IL-13.<sup>29</sup> These results are consistent with previous studies that IL-13 plays a role in the pathogenesis of pulmonary inflammation and alveolar remodeling after exposure to coal dust and provide evidence that polarization of Th2 cells involving IL-13 can support the development of pulmonary fibrosis.<sup>30</sup> Blocking the IL-13R $\alpha$ 2 signal

decreases collagen deposition in bleomycin-induced fibrosis.<sup>31</sup> In vitro, IL-13 activates epithelial cells, and then activation of epithelial cells releases growth factors such as TGF- $\beta$  and enhances the regulation of collagen type I production.<sup>29</sup> The transition metal content within the coal dust probably causes the effects of coal dust in causing airway remodeling by stimulating cytokines production. According to a scientific study, mineral dust can directly produce fibrosis in the airway wall.<sup>32</sup> Minerals like Cd, Cu, and Se are positively related to asthma exacerbations.<sup>33</sup>

#### **Effect of IL-13 lung tissue on bronchial and bronchiole the number of goblet cells after exposure to coal dust in an asthma mice model**

Hyperplasia and hypertrophy of goblet airway cells are features of airway remodeling in asthma related to airway protection and allergen removal.<sup>3</sup> The immunological response is correlated with an augmentation in the quantity of goblet cells of Th2 cells, mainly controlled by IL-13 and IL-4 in asthma. This study showed no positive and significant effect between IL-13 lung tissue and increased goblet cells after exposure to coal dust in asthma mice models. The possible reason for the variation in goblet cell count, regardless of IL-13, could be the interaction between the asthma mice model and coal dust. Coal dust causes pathology in the lungs. Severe pulmonary remodeling due to coal dust exposure in an asthma mouse model can trigger goblet cell responses, regardless of IL-13 signals during sub-chronic exposure to coal dust. This study's results align with those of Ge et al., who stated that other cytokines from Th2 may stimulate goblet cell proliferation, such as IL-9 and IL-5. IL-9 and IL-5 directly induce goblet cell hyperplasia without IL-13 dependence on a mouse model-induced chronic allergen exposure.<sup>34</sup> These data demonstrate that airway goblet cell hyperplasia can be independent of IL-13 associated with the OVA + coal dust combination.

This study established the effects of respiratory coal dust particles on lung epithelial and inflammatory cells in mice asthma models, but it had some limitations. We only examined differentiation between two groups, OVA and OVA + Coal dust group, and did not compare with the coal dust group alone. In future studies, it would be interesting to compare the effects of coal dust only on tissue damage and the biomarkers associated with Eosinophil and IL-13. Our study also was based on a mouse model of asthma; in the future, we plan to confirm the molecular mechanism in human pneumoconiosis.

#### **CONCLUSION**

Coal dust is a pollutant particle that can potentially increase the severity of airway remodeling in animal models induced by OVA through the indirect effect of eosinophils via IL-13 and the direct effect of IL-13 on the epithelium and subepithelial fibrosis thickness. The results of this study are hoped to serve as a rationalization for coal pneumoconiosis management and prevention, as well as a starting point for future studies.

#### **ACKNOWLEDGMENTS**

The author would like to thank those who helped implement this research, especially Mr. Wahyudha Ngatiril Lady, S.Si. (Biomedical central laboratory analyst) and Mr. Mochamad Abuhari (Pharmacology laboratory analyst) at Faculty of Medicine, Universitas Brawijaya.

#### **REFERENCES**

1. James AL, Donovan GM, Green FHY, et al. Heterogeneity of Airway Smooth Muscle Remodelling in Asthma. *Am J Respir Crit Care Med* 2022. doi: 10.1164/rccm.202111-2634OC.
2. Ram A, Mabalirajan U, Jaiswal A, et al. Parabromophenacyl bromide inhibits subepithelial fibrosis by reducing TGF- $\beta$ 1 in a chronic mouse model of allergic asthma. *Int Arch Allergy Immunol* 2015;167(2):110–118. doi: 10.1159/000434679.
3. Huang Y, Qiu C. Research advances in airway remodeling in asthma: a narrative review. *Ann Transl Med* 2022;10(18):1023–1023. doi: 10.21037/atm-22-2835.
4. Hussain M, Liu G. Eosinophilic Asthma: Pathophysiology and Therapeutic Horizons. *Cells* 2024, Vol 13, Page 384 2024;13(5):384. doi: 10.3390/CELLS13050384.
5. Cusack RP, Whetstone CE, Xie Y, et al. Regulation of eosinophilia in asthma—new therapeutic approaches for asthma treatment. *Cells* 2021;10(4). doi: 10.3390/cells10040817.
6. Pfeffer PE, Mudway IS, Grigg J. Air Pollution and Asthma – Mechanisms of Harm and Considerations for Clinical Interventions. *Chest* 2021;159(4):1346–55. doi: 10.1016/j.chest.2020.10.053
7. Tétreault LF, Doucet M, Gamache P, et al. Childhood exposure to ambient air pollutants and the onset of asthma: An administrative cohort study in Québec. *Environ Health Perspect* 2016;124(8):1276–1282. doi: 10.1289/ehp.1509838.
8. Vanka KS, Shukla S, Gomez HM, et al. Understanding the pathogenesis of occupational coal and silica dust-associated lung disease. *European Respiratory Review* 2022;31(165). doi: 10.1183/16000617.0250-2021.
9. Sun Y, S.Kinsela A, David Waite T. Elucidation of alveolar macrophage cell response to coal dusts: Role of ferroptosis in pathogenesis of coal workers' pneumoconiosis. *Science of The Total Environment* 2022;823. doi:10.1016/j.scitotenv.2022.153727
10. Kania N, Setiawan B, Widjajanto E, et al. Peroxidative index as novel marker of hydrogen peroxide involvement in lipid peroxidation from coal dust exposure. *Oxid Antioxid Med Sci* 2012;1(3):209. doi: 10.5455/oams.031012.or.020.
11. Zhang Y, Li A, Gao J, et al. Differences in the characteristics and pulmonary toxicity of nano- and micron-sized respirable coal dust. *Respir Res* 2022;23(1):1–18. doi: 10.1186/s12931-022-02120-8.



12. Hidayat T, Yuliarto S, Barlianto W, et al. Increase of Bcl-2/Bax ratio corelated with decrease of lymphocyte apoptosis: A study in the bronchiolus and lung of asthmatic mice. *International Journal of Medicine and Medical Sciences* 2013;5(4):191–197. doi: 10.5897/IJMS2012.0873.
13. Budianto WY, Khotimah H, Suhartono E. Effect of coal dust exposure on the SOD activity and the oxidative DNA damage in asthmatic mice. *Indonesian Biomedical Journal* 2019;11(2):159–166. doi: 10.18585/inabj.v11i2.579.
14. Weller PF, Spencer LA. Functions of tissue-resident eosinophils. *Nat Rev Immunol* 2017;17(12):746–760. doi: 10.1038/nri.2017.95.
15. Guthier HE, Zimmermann N. Targeting Eosinophils in Mouse Models of Asthma. *Methods Mol Biol* 2022;2506:211–222. doi: 10.1007/978-1-0716-2364-0\_15.
16. Nakagome K, Nagata M. Involvement and Possible Role of Eosinophils in Asthma Exacerbation. *Front Immunol* 2018;9. doi: 10.3389/FIMMU.2018.02220.
17. Kanda A, Fleury S, Kobayashi Y, et al. Th2-activated eosinophils release Th1 cytokines that modulate allergic inflammation. *Allergol Int* 2015;64 Suppl:S71–S73. doi: 10.1016/J.ALIT.2015.03.006.
18. Huang WC, Liu CY, Shen SC, et al. Protective effects of licochalcone a improve airway hyper-responsiveness and oxidative stress in a mouse model of asthma. *Cells* 2019;8(6). doi: 10.3390/cells8060617.
19. Hasan AA, Azawi IH, A-Al-hilali H. Cysteine leukotriene receptors type 2 (CyLTR2 M01 V) gene polymorphism and its role in iraqi asthmatic patients. *Res J Pharm Technol* 2019;12(9):4125–4128. doi: 10.5958/0974-360X.2019.00712.1.
20. Hur J, Kang JY, Rhee CK, et al. The leukotriene receptor antagonist pranlukast attenuates airway 2 remodeling by suppressing TGF- $\beta$  signaling. *Pulm Pharmacol Ther* 2017;Feb(48):5–14. doi: 10.1016/j.pupt.2017.10.007.
21. Janulaityte I, Januskevicius A, Kalinauskaite-Zukauske V, et al. In vivo allergen-activated eosinophils promote collagen I and fibronectin gene expression in airway smooth muscle cells via TGF- $\beta$ 1 signaling pathway in Asthma. *Int J Mol Sci* 2020;21(5):1–19. doi: 10.3390/ijms21051837.
22. Travers J, Rothenberg ME. Eosinophils in mucosal immune responses. *Mucosal Immunol* 2015;8(3):464–475. doi:10.1038/mi.2015.2.
23. Katoh S, Matsumoto N, Tanaka H, et al. Elevated levels of periostin and TGF- $\beta$  1 in the bronchoalveolar lavage fluid of patients with idiopathic eosinophilic pneumonia. *Asian Pac J Allergy Immunol* 2020;38:208–213. doi: 10.12932/AP-111018-0414.
24. Everman JL, Rios C, Seibold MA. Chapter 30 Model to Assess Primary Airway Epithelial Cell Responses. In: *Type 2 Immunity* Springer; 2018; pp. 419–432. doi: 10.1007/978-1-4939-7896-0.
25. Yang SJ, Allahverdian S, Saunders ADR, et al. IL-13 signaling through IL-13 receptor  $\alpha$ 2 mediates airway epithelial wound repair. *FASEB Journal* 2019;33(3):3746–3757. doi: 10.1096/fj.201801285R.
26. Michalik M, Wójcik-Pszczola K, Paw M, et al. Fibroblast-to-myofibroblast transition in bronchial asthma. *Cellular and Molecular Life Sciences* 2018;75(21):3943–3961. doi: 10.1007/s00018-018-2899-4.
27. Al-Azzam N, Elsalem L. Leukotriene D4 role in allergic asthma pathogenesis from cellular and therapeutic perspectives. *Life Sci* 2020;260(August):118452. doi: 10.1016/j.lfs.2020.118452.
28. Yu J, Li K, Xu J. Indoor PM2.5 from coal combustion aggravates ovalbumin-induced asthma-like 2 airway inflammation in BALB/c mice. *Am J Physiol Lung Cell Mol Physiol* 2019;317(1):L29–L3. doi: 10.1152/ajplung.00012.2019.
29. Nakagome K, Nagata M. The Possible Roles of IL-4/IL-13 in the Development of Eosinophil-Predominant Severe Asthma. *Biomolecules* 2024, Vol 14, Page 546 2024;14(5):546. doi: 10.3390/BIOM14050546.
30. Wang Z, Ji N, Chen Z, et al. MiR-1165-3p suppresses Th2 differentiation via targeting IL-13 and PPM1A in a mouse model of allergic airway inflammation. *Allergy, Asthma & Immunology Research*. 2020 Sep;12(5):859. *Allergy Asthma Immunol Res* 2020;12(5):859–876. doi:10.4168/air.2020.12.5.859.
31. Nie Y, Hu Y, Yu K, et al. Akt1 regulates pulmonary fibrosis via modulating IL-13 expression in macrophages. *Innate Immun* 2019;25(7):451–461. doi: 10.1177/1753425919861774.
32. Elhadidy MG, Elmasry A, Elsayed HRH, et al. Modulation of Cox-2 And NADPH Oxidase-4 By Alpha-Lipoic Acid Ameliorates Busulfan-Induced Pulmonary Injury In Rats. *Heliyon* 2021;7(10):e08171. doi: 10.1016/j.heliyon.2021.e08171.
33. Huang X, Xie J, Cui X, et al. Association between concentrations of metals in urine and adult asthma: A case-control study in Wuhan, China. *PLoS One* 2016;11(5):1–18. doi: 10.1371/journal.pone.0155818.
34. Ge Y, Cheng R, Sun S, et al. Fangxiao Formula alleviates airway inflammation and remodeling in rats with asthma via suppression of transforming growth factor- $\beta$ /Smad3 signaling pathway. *Biomedicine and Pharmacotherapy* 2019;119(September):109429. doi: 10.1016/j.biopha.2019.109429.



# JOURNAL OF BIOMEDICINE AND TRANSLATIONAL RESEARCH

Available online at JBTR website: <https://jbtr.fk.undip.ac.id>

Copyright©2024 by Faculty of Medicine Universitas Diponegoro, Indonesian Society of Human Genetics and Indonesian Society of Internal Medicine

Original Research Article

## Long-Term Effects of Low-Dose Chlorpyrifos Exposure on Serum Albumin Levels in Male Wistar Rats

Desie Dwi Wisudanti<sup>1\*</sup>, Noval Hidayat<sup>2</sup>, Muhammad Afiful Jauhani<sup>3</sup>

<sup>1</sup>Department of Pharmacology, Faculty of Medicine, Universitas Jember, Indonesia

<sup>2</sup>Faculty of Medicine, Universitas Jember, Indonesia<sup>3</sup>

<sup>3</sup>Department of Forensic and Medicolegal, Faculty of Medicine, Universitas Jember, Indonesia

### Article Info

History

Received: 12 Mar 2024

Accepted: 12 Oct 2024

Available: 30 Dec 2024

### Abstract

**Background:** Chlorpyrifos is one of the organophosphate pesticide types frequently utilized as a pest control agent in Indonesia. Despite its effectiveness in combating pests, the residue levels of chlorpyrifos in the environment and plants have raised serious concerns. Long-term accumulation of chlorpyrifos in the body can lead to organ damage, particularly in the liver and kidneys, which may decrease serum albumin levels.

**Objective:** To investigate the impact of low-dose chlorpyrifos exposure over time on serum albumin levels in Wistar rats.

**Methods:** This study used a posttest-only randomized control group design method, conducted from May until September 2023. Thirty male Wistar rats were divided into five groups: the normal control group (Kn) received normal saline solution (+5% Tween 20) orally for 56 days, while the treatment groups (K1, K2, K3, and K4) were administered chlorpyrifos at a dose of 5 mg/kg body weight for 7 days, 14 days, 28 days, and 56 days orally. Serum albumin levels were measured using the dye-binding method with a spectrophotometer.

**Results:** The measurement results indicate that the normal control group (Kn) had the highest serum albumin levels ( $4.326 \pm 0.519$  g/dL). Serum albumin levels decreased in the groups treated with chlorpyrifos. The longer the chlorpyrifos exposure, the lower the serum albumin levels. The lowest serum albumin levels were found in group K4 with chlorpyrifos exposure for 56 days ( $2.826 \pm 0.358$  g/dL). Statistical analysis using One-way ANOVA and Post Hoc LSD tests showed significant differences ( $p < 0.05$ ) between all treatment groups (K1, K2, K3, and K4) and the control group (Kn).

**Conclusion:** This study shows that administering low-dose chlorpyrifos over a period of 7 to 56 days has a significant effect in reducing serum albumin levels in Wistar rats. The clinical implications of this decrease in serum albumin levels need to be considered in the context of exposure to organophosphate pesticide residues in humans.

**Keywords:** Organophosphates; hepatic toxicity; proteins; pesticide residues.

**Permalink/ DOI:** <https://doi.org/10.14710/jbtr.v10i3.22240>

### INTRODUCTION

Organophosphates are the most widely used type of pesticide in the world due to their effectiveness in eradicating agricultural pests.<sup>1</sup> One of the organophosphate pesticides frequently used in Indonesia is chlorpyrifos.<sup>2</sup> Chlorpyrifos accounts for 40% of the total organophosphate pesticides used.<sup>3</sup> The effectiveness of chlorpyrifos in pest eradication is proportional to the residue it generates in the

environment and plants. A study revealed that using chlorpyrifos in agriculture leads to chlorpyrifos residues in soil exceeding the maximum pesticide residue.<sup>2</sup> Long-term residue exposure can lead to the accumulation of chlorpyrifos in the body, resulting in symptoms of chlorpyrifos toxicity.<sup>4</sup>

\*Corresponding author:

E-mail: [desie.fk@unej.ac.id](mailto:desie.fk@unej.ac.id)

(Desie Dwi Wisudanti)

Long-term accumulation of chlorpyrifos can damage various organs, including the nervous, cardiovascular, respiratory, liver, and kidneys.<sup>4</sup> Studies indicate that administration of 1 mg/kg BW of sub-chronic chlorpyrifos to experimental animals for 90 days damaged hepatocytes.<sup>5,6</sup> The metabolic process of chlorpyrifos by esterase and cytochrome P450 enzymes in the liver produces more toxic compounds, namely chlorpyrifos-oxon, and 3,4,5-trichloro-2-pyridinol causing oxidative stress and triggering liver cell damage.<sup>7,8</sup> Liver cell damage also results in decreased albumin production, causing hypoalbuminemia.<sup>5</sup> Additionally, the effects of long-term accumulation of chlorpyrifos in the body can also cause kidney damage.<sup>7</sup> Chlorpyrifos is excreted from the body through the kidneys in the form of 3,5,6-trichloro-2-pyridinol (TCP), a metabolite that is more soluble in air and can be easily excreted by the kidneys into the urine.<sup>9</sup> Accumulation of TCP in the kidneys can cause oxidative stress on glomerular epithelial cells, triggering damage to epithelial cells in the glomerulus.<sup>7</sup> Damage to the glomerular epithelium can interfere with the ability to filter substances visually so that albumin and other proteins can leak into the urine and cause hypoalbuminemia.<sup>10</sup>

Hypoalbuminemia can impact various bodily functions, including systemic edema and pleural effusion, due to decreased oncotic pressure in the blood vessels. Hypoalbuminemia can also interfere with transporting various hydrophobic molecules, such as lipid-derived hormones (thyroid, estrogen, testosterone, and cortisol), lipid-based drugs, and other air-insoluble ions.<sup>11</sup> Hypoalbuminemia also impacts decreased cell regeneration ability, reduced immunity, and impaired neutralization of free radicals.<sup>12</sup>

The results of research on the effect of chlorpyrifos on albumin levels in rats are still limited<sup>13</sup>, more often carried out on fish as experimental animals.<sup>14–16</sup> Those studies showed decreased albumin levels in the group given chlorpyrifos. In a study conducted by Ravikumar et al. (2020), Wistar rats were given chlorpyrifos at a high dose of 25 mg/kg BW for 28 days, and albumin levels were checked on the 15th and 29th days. The study results showed a significant decrease ( $p < 0.05$ ) in total protein and albumin levels in the group given chlorpyrifos on the 15th and 29th days of the experiment.<sup>13</sup> Studies on organophosphate poisoning patients showed symptoms of hypoalbuminemia in those poisoned by chlorpyrifos.<sup>8</sup>

Studies in mammalian animals have focused more on liver and kidney cell damage caused by chlorpyrifos, and the results have had different effects on these organs. In addition, these studies have not provided much data on the decrease in albumin levels caused by chlorpyrifos. Administration of a low dose of chlorpyrifos (2 mg/kg BW) for 12 hours in rats causes an oxidative stress response in the liver.<sup>17</sup> There were no changes in liver histology in rats at low doses (1 mg/kg BW) for 12 weeks.<sup>6</sup> High doses of chlorpyrifos (50 mg/kg BW) for 4 weeks showed proliferation of Kupffer cells in the liver and local bleeding in the kidneys.<sup>7</sup>

Research on administering low doses of chlorpyrifos over various periods in the same study is still limited. In *Esisenia fetida*, an earthworm species, chlorpyrifos

toxicity was lower after 28 days compared to groups exposed to other compounds but higher after 56 days of administration.<sup>18</sup>

Therefore, using a time-series study design, research on albumin in long-term low-dose chlorpyrifos administration can help identify possible impacts over a more extended period. By monitoring albumin levels over time, it can be seen whether low-dose chlorpyrifos administration can cause significant changes in albumin levels. This study is expected to provide new insights into the potential side effects of chlorpyrifos on the systemic body, especially in the context of albumin levels.

## MATERIALS AND METHODS

### Research Design and Experimental Animal

This research was conducted after obtaining ethical approval from the Health Research Ethics Commission of the Faculty of Medicine, University of Jember, with approval number 1813/H25.1.11/KE/2023. The research used a posttest-only randomized control group design method. A total of 30 healthy white male rats of the Wistar strain (*Rattus norvegicus*) aged 2-3 months, weighing 150-200 g, were randomly divided based on weight into five groups, with six rats each. The number of samples for each group was calculated using the resource equation method and correction factor to anticipate dropout. The five groups were the normal control group given 5 mL/kg BW saline (+5% Tween 20) orally for 56 days (K), the chlorpyrifos group 5 mg/kg BW orally for 7 days (P1), 14 days (P2), 28 days (P3), and 56 days (P4). The animals were kept in full hygienic conditions and had free access to fresh water and standard pellets. This study was conducted from May until September 2023 in the experimental animal house, Pharmacology Laboratory, and Clinical Pathology Laboratory Faculty of Medicine, University of Jember.

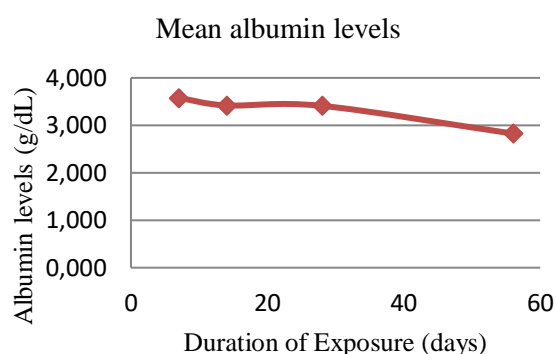


**Figure 1.** Graph of albumin levels according to duration of exposure

**Table 1.** Measurement of Serum Albumin Levels

Group	Mean Serum Albumin Levels (g/dL) (Mean±standard deviation)
Kn	4,326±0,519
K1 (7 days)	3,578±0,599
K2 (14 days)	3,42±0,704
K3 (28 days)	3,41±0,481
K4 (56 days)	2,826±0,358

**Table 2.** Results of Post Hoc LSD Test

	<b>Kn</b>	<b>K1</b>	<b>K2</b>	<b>K3</b>	<b>K4</b>
Kn		0,025*	0,008*	0,007*	0,000**
K1	0,025*		0,619	0,597	0,025*
K2	0,008*	0,619		0,975	0,071
K3	0,007*	0,597	0,975		0,076
K4	0,000**	0,025*	0,071	0,076	

Explanation: (\*) indicates significant difference ( $p < 0.05$ ), (\*\*) indicates highly significant difference ( $p < 0.001$ )

### Materials

This study used chlorpyrifos pestanal analytical standard (Sigma-Aldrich), saline, Tween 20, distilled water, reagen BCG Albumin (Dialab), and 30 male Wistar rats.

### Preparation of Chlorpyrifos Solution

Chlorpyrifos solution 5 mg/kg BW (1/30 LD50) was made by weighing chlorpyrifos. After that, it was mixed with Tween 20, and then saline was added and stirred until evenly mixed.

### Albumin Level Examination

After the treatment, the rats were terminated using intraperitoneal injection of pentobarbital at a dose of 200 mg/kg BW, and their blood was taken intracardially to examine serum albumin levels. Serum preparation began with incubation of rat blood for 10-20 minutes, then centrifugation was carried out at a speed of 3000 rpm for 10 minutes. The blood serum was separated from the solution and then put into micro tubes and labeled. Before serum albumin level examination, blank reagent and standard reagent were prepared by inserting 5  $\mu$ L of distilled water and 500  $\mu$ L of BCG reagent into the blank tube, and 5  $\mu$ L of standard solution and 500  $\mu$ L of BCG reagent into the standard tube. Serum albumin sample examination was done using the dye-binding method by inserting 5  $\mu$ L of blood serum and 500  $\mu$ L of BCG reagent into the sample tube.<sup>19</sup> All solutions were homogenized using a vortex and incubated for 10 minutes at 20-25 degrees Celsius. Albumin level readings were carried out by measuring the absorbance value of the solution using a spectrophotometer with a wavelength of 546 nm.

### Statistical Analysis

The research data obtained were presented in tables and processed using One Way ANOVA statistical analysis with a confidence level of 95% ( $\alpha = 0.05$ ), then continued with the Post Hoc LSD difference test.

## RESULTS

The results of serum albumin levels measurement and the graph of albumin levels according to the duration of exposure are shown in Table 1 and Figure 1, respectively. Based on the average serum albumin levels measured in each group, it was found that the Kn group had the highest albumin levels compared to the other groups, at  $4.326 \pm 0.519$  g/dL. The lowest albumin levels were observed in group K4, which received chlorpyrifos for 56 days at  $2.826 \pm 0.358$  g/dL. The albumin levels from K1 to K4 showed a decreasing trend, indicating that

with prolonged exposure to chlorpyrifos, the albumin levels in rats also decreased.

The obtained serum albumin level results were further subjected to comparative analysis using One-way ANOVA. The requirement for the one-way ANOVA test to be carried out is that the data must be normally distributed and homogeneous. Therefore, the data was previously analyzed using the Shapiro-Wilk normality test and the homogeneity test using the Levene test. The results of the normality and homogeneity tests of the data obtained  $p > 0.05$ , which means that the data is normally distributed and homogeneous so that it can be continued with the one-way ANOVA test. Based on the One-way ANOVA test, a significance result of 0.002 ( $p < 0.05$ ) was obtained. The analysis was continued with the Post Hoc LSD test. The results of the Post Hoc LSD test (Table 2) showed a significant difference ( $p < 0.05$ ) in serum albumin levels between the control group (Kn) and the chlorpyrifos-exposed groups (K1, K2, K3, and K4), as well as between group K1 and K4. This difference can be attributed to the varying exposure durations, especially between K1 exposed for 7 days and K4 exposed for 56 days. The difference in exposure durations provides an insight into the accumulation of significant effects of chlorpyrifos exposure on serum albumin levels, thus demonstrating that with prolonged (chronic) exposure to chlorpyrifos, serum albumin levels will also decrease.

## DISCUSSION

This study aims to prove the effect of low-dose chlorpyrifos administration on albumin levels in Wistar rats, using a time series, namely administration in 7, 14, 28 and 56 days. These times were chosen to represent acute (7 days), subacute (14 days), and subchronic (28 and 56 days) toxicity in animal toxicity assessment.<sup>20</sup> A low dose of chlorpyrifos was given to resemble the residual dose found in vegetables and fruits consumed by humans, considering that chlorpyrifos is often used in agriculture, especially to control pests in vegetable and fruit products.<sup>21</sup> Chlorpyrifos has an oral LD50 in rats ranging from 66-195 mg/kg BW or 150 mg/kg BW.<sup>22,23</sup> It is stated in research conducted by Noushi (2013) that a low dose is 1/30 of the LD50, so from the LD50, the dose range that can be used is 2.2 - 6.5 mg/kg BW or 5 mg/kg BW.<sup>24</sup>

Our study showed that the group given low-dose chlorpyrifos 5 mg/kg BW for 7, 14, 28, and 56 days had significantly lower serum albumin levels compared to the group not given chlorpyrifos. Normal albumin levels in male Wistar rats are 3-5.1 g/dL, and the group not given chlorpyrifos had albumin levels of  $4.236 \pm 0.519$  g/dL, indicating that the levels were within the normal range.

In this study, it was found that the average albumin levels decreased in the group given chlorpyrifos, starting on the seventh day of treatment, namely  $3.578 \pm 0.599$  g/dL, and the lowest on the 56th day was  $2.826 \pm 0.358$  g/dL. A retrospective study by Noh *et al.* (2020) investigating the effects of organophosphate poisoning on 217 patients showed the presence of hypoalbuminemia. The study examined several organophosphates that were accidentally ingested, categorized as low dose (2 mg/kg body weight) and high dose ( $> 2$  mg/kg body weight), followed by observation after 24 hours.<sup>8</sup> The doses are doses in humans, where the dose used in our study was a low dose after being converted to humans, which was 0.8 mg/kg BW ( $\leq 2$  mg/kg BW). From Noh's study, organophosphates were shown to trigger an oxidative stress response in the liver, which can result in reduced albumin production.<sup>8</sup>

In this study, the exposure of low-dose chlorpyrifos was found to significantly decrease serum albumin levels, with an average of  $3.41 \pm 0.481$  g/dL at 28 days and a further decrease at 56 days with an average of  $2.826 \pm 0.358$  g/dL. This effect is believed to occur due to the accumulation effect of low doses of chlorpyrifos, causing increasingly severe hepatocyte damage resulting in decreased albumin production. In contrast, a study by Zhang *et al.* (2021) found that exposure to low-dose chlorpyrifos (1 mg/kg body weight) for 12 weeks did not show any significant changes in liver histological examination in rats.<sup>6</sup> This is because the dose exhibited significant hepatotoxicity in that study was 5.4 mg/kg body weight, leading to hepatotoxicity through changes in liver enzyme markers' profiles such as ALP, AST, LDH, and organ structure. Chlorpyrifos can elevate TNF $\alpha$ , IL-1 $\beta$ , and IL-6 levels and induce inflammatory responses with increasing doses.<sup>6</sup>

The metabolism of chlorpyrifos in the liver through hydrolysis by esterase enzymes and cytochrome P450 results in the formation of a more toxic compound called chlorpyrifos-oxon (CPO), which triggers liver cell damage through oxidative stress mechanisms. Liver cell damage affects the physiological function of the liver, one of which is the production of albumin protein. Research indicates that the decrease in serum albumin levels correlates with the degree of hepatocyte damage.<sup>25</sup> Such a condition can exacerbate the development of hypoalbuminemia resulting from chlorpyrifos exposure.<sup>8</sup>

Exposure to chemical substances such as chlorpyrifos can trigger oxidative stress in the liver, primarily due to the high production of reactive oxygen species (ROS), especially from mitochondria and NADPH oxidase. Elevated ROS levels can cause damage to liver cell components, including lipids, proteins, and nucleic acids. Additionally, oxidative stress can disrupt normal mitochondrial function, altering energy production processes within liver cells and leading to structural and functional changes in the liver that can affect overall organ performance. One consequence of this oxidative stress is the reduction in albumin production by the liver, leading to hypoalbuminemia. Therefore, oxidative stress plays a key role in the mechanism of liver damage and the decrease in albumin levels.<sup>26,27</sup>

Oxidative stress due to chlorpyrifos exposure leads to changes in metabolic function, ultimately resulting in cell death. The mechanism of non-cholinergic pro-oxidant effects on chlorpyrifos and chlorpyrifos-oxon (CPO) toxicity has been studied by Naime *et al.* (2020).<sup>28</sup> Exposure to chlorpyrifos and chlorpyrifos-oxon (CPO) results in a significant decrease in glutathione levels, preceding a significant reduction in cell viability. The study indicates that, apart from being a stronger acetylcholinesterase inhibitor, chlorpyrifos-oxon is also a potent pro-oxidant molecule. Thus, oxidative injury can contribute to liver and kidney damage as the human liver expresses CYP2B6, the main enzyme responsible for chlorpyrifos metabolism, into chlorpyrifos-oxon. Additionally, subacute exposure to low doses forms toxic oxon metabolites, causing hyalinization, vacuolization, nuclear necrosis, hepatocyte edema, and lipid degeneration. These morphological changes may also be associated with impaired cell function and lower antioxidant capacity.<sup>28,29</sup>

Apart from liver cell damage, hypoalbuminemia can also occur due to kidney damage. Research conducted by Sakinah *et al.* in 2024 showed that oral administration of low-dose chlorpyrifos pesticides in 7, 14, 28 and 56 days can cause increased BUN and creatinine levels and decreased glomerular diameter in the group given chlorpyrifos compared to the group without chlorpyrifos.<sup>30</sup> A study by Aung *et al.* (2022) investigated the exposure of chlorpyrifos to kidney damage in 18 rats treated with subacute and subchronic doses of 18 mg/kg body weight via subcutaneous injection. From the study, kidney damage was observed through oxidative stress processes. One of the most well-known mechanisms of organophosphate pesticide-induced kidney damage in subacute and subchronic exposure is through oxidative stress effects on the kidneys. Malondialdehyde (MDA) is a product of lipid peroxidation and is considered an oxidative marker. The results of the study indicated significant changes in oxidative damage as the basis of nephrotoxicity, as serum MDA levels increased and were strongly expressed in renal tubular cells in animals exposed to chlorpyrifos.<sup>31</sup>

Accumulation of 3,4,5-trichloro-2-pyridiol in the kidney can induce oxidative stress in glomerular epithelial cells, damaging the glomeruli's visceral epithelial cells (podocytes).<sup>7</sup> Damage or abnormalities in glomerular podocytes can disrupt their ability to filter substances selectively. As a result, albumin and other proteins may leak into the urine.<sup>32</sup> When the amount of albumin lost in the urine exceeds the liver's capacity to replace the loss, the level of albumin in the plasma decreases (hypoalbuminemia).<sup>33</sup>

One of the factors that can affect albumin levels is the age of the rats. In the study of Olukuran (2018), it was shown that there was a relationship between changes in urinary protein excretion in rats at various ages. The study proved that some of the molecular weight of protein in the urine of rats aged 1, 9, and 12 months was higher than that of rats aged 3 and 6 months. The total protein concentration in the urine of male and female rats aged 9 and 12 months was significantly higher than that of rats aged 1 and 3 months.<sup>34</sup> In our study, we used rats aged 2-3 months. Thus, selecting 2-3-month-old rats should not affect albumin levels in the rats we studied.

Our study has limitations: albumin levels were not checked at hour 0 to ensure that all groups had the same albumin levels before chlorpyrifos administration. However, albumin levels in the treatment group were compared with normal control groups that were not given chlorpyrifos. So, by including the same age in the research inclusion criteria, getting the same type of food, and using the same environmental conditions, it is expected to reduce the possibility of bias in this study that can affect the study results. The results of this study can be the basis for further research, for example, on the effect of chlorpyrifos on drug pharmacokinetics, especially in terms of drug distribution bound to albumin.

## CONCLUSION

This study concluded that the duration of low-dose chlorpyrifos exposure can cause changes in serum albumin levels in Wistar rats. Albumin levels in the chlorpyrifos administration group were significantly lower than those without chlorpyrifos. This result proves that the longer the organism is exposed to low-dose chlorpyrifos pesticides, the lower the organism's albumin levels.

## ACKNOWLEDGMENTS

We would like to express our gratitude to the Faculty of Medicine, Universitas Jember, for facilitating this research. Additionally, we extend our thanks to LP2M Universitas Jember for providing research funding through the KeRis DiMas program.

## REFERENCES

- Thakur M, Medintz IL, Walper SA. Enzymatic Bioremediation of Organophosphate Compounds—Progress and Remaining Challenges. *Front Bioeng Biotechnol*. 2019 Nov 8;7:488078. doi: 10.3389/fbioe.2019.00289
- Supriyanto S, Nurhidayanti N, Pratama HF. Dampak Cemaran Residu Klorpirifos Terhadap Penurunan Kualitas Lingkungan pada Lahan Pertanian. *Jurnal Tekno Insentif Insentif*. 2021 Apr 30;15(1):30–40. doi: 10.36787/jti.v15i1.395
- Liem JF, Mansyur M, Soemarmo DS, Kekalih A, Subekti I, Suyatna FD, et al. Cumulative exposure characteristics of vegetable farmers exposed to Chlorpyrifos in Central Java – Indonesia; a cross-sectional study. *BMC Public Health* 2021 Dec 5;21(1):1–9. doi: 10.1186/s12889-021-11161-5
- Wołejko E, Łozowicka B, Jabłońska-Trypuc A, Pietruszyńska M, Wydro U. Chlorpyrifos Occurrence and Toxicological Risk Assessment: A Review. *Int J Environ Res Public Health*. 2022 Sep 26;19(19):12209. doi: 10.3390/ijerph191912209
- Kaur M, Jindal R. Oxidative stress response in liver, kidney and gills of ctenopharyngodon idellus (cuvier & valenciennes) exposed to chlorpyrifos. *MOJ Biology and Medicine*. 2017 Jul 20;1(4). doi: 10.15406/mojbm.2017.01.00021
- Zhang Y, Jia Q, Hu C, Han M, Guo Q, Li S, et al. Effects of chlorpyrifos exposure on liver inflammation and intestinal flora structure in mice. *Toxicol Res (Camb)*. 2021;10(1):141–9. doi: 10.1093/toxres/tfaa108
- Deng Y, Zhang Y, Lu Y, Zhao Y, Ren H. Hepatotoxicity and nephrotoxicity induced by the chlorpyrifos and chlorpyrifos-methyl metabolite, 3,5,6-trichloro-2-pyridinol, in orally exposed mice. *Sci Total Environ*. 2016 Feb 15;544:507–14. doi: 10.1016/j.scitotenv.2015.11.162
- Noh E, Moon JM, Chun BJ, Cho YS, Ryu SJ, Kim D. The clinical role of serum albumin in Organophosphate poisoning. *Basic Clin Pharmacol Toxicol*. 2021 Apr 1;128(4):605–14. doi: 10.1111/bcpt.13546
- Liu HF, Ku CH, Chang SS, Chang CM, Wang IK, Yang HY, et al. Outcome of patients with chlorpyrifos intoxication. 2020 Apr 27;39(10):1291–300. doi: 10.1177/0960327120920911
- Benzing T, Salant D. Insights into Glomerular Filtration and Albuminuria. *New England Journal of Medicine*. 2021 Apr 15;384(15):1437–46. doi: 10.1056/NEJMr1808786
- Soeters PB, Wolfe RR, Shenkin A. Hypoalbuminemia: Pathogenesis and Clinical Significance. *JPEN J Parenter Enteral Nutr*. 2019 Feb 1;43(2):181–93. doi: 10.1002/jpen.1451
- Lantigua D, Nguyen MA, Wu X, Suvarnapathaki S, Kwon S, Gavin W, et al. Synthesis and characterization of photocrosslinkable albumin-based hydrogels for biomedical applications. *Soft Matter*. 2020 Oct 21;16(40):9242–52. doi: 10.1039/d0sm00977f
- Rao P, Ravikumar Y, Madhuri D, Lakshman M, Reddy AG, Kalakumar B. Article in *Toxicology International*. 2020. doi: 10.18311/ti/2022/v29i4/30251
- Abdel-Daim MM, Dawood MAO, Elbadawy M, Aleya L, Alkahtani S. Spirulina platensis Reduced Oxidative Damage Induced by Chlorpyrifos Toxicity in Nile Tilapia (*Oreochromis niloticus*). *Animals*. 2020 Mar;10(3):473. doi: 10.3390/ani10030473
- Mansour AT, Hamed HS, El-Beltagi HS, Mohamed WF. Modulatory Effect of Papaya Extract against Chlorpyrifos-Induced Oxidative Stress, Immune Suppression, Endocrine Disruption, and DNA Damage in Female Clarias gariepinus. *International Journal of Environmental Research and Public Health*. 2022 Apr 12;19(8):4640. doi: 10.3390/ijerph19084640
- Chhaba B, Dhamagaye HB, Pawase AS, Sapkale PH, Chavan BR, Meshram SJ, et al. The Short-term Exposure Effect of Chlorpyrifos (20% EC) on Haematological, Biochemical and Histopathological Response of Striped Catfish *Pangasianodon hypophthalmus*. *Turk J Fish Aquat Sci*. 2024 Jul 3;24(10). doi: 10.4194/TRJFAS24608
- Kondakala S, Lee JH, Ross MK, Howell GE. Effects of acute exposure to chlorpyrifos on cholinergic and non-cholinergic targets in normal and high-fat fed male C57BL/6J mice. *Toxicol Appl Pharmacol*. 2017 Dec;337:67–75. doi: 10.1016/j.taap.2017.10.019

18. Hou K, Yang Y, Zhu L, Wu R, Du Z, Li B, et al. Toxicity evaluation of chlorpyrifos and its main metabolite 3,5,6-trichloro-2-pyridinol (TCP) to *Eisenia fetida* in different soils. *Comparative Biochemistry and Physiology Part C: Toxicology & Pharmacology*. 2022 Sep 1;259:109394.
19. Oviedo MJ, Quester K, Hirata GA, Vazquez-Duhalt R. Determination of conjugated protein on nanoparticles by an adaptation of the Coomassie blue dye method. *MethodsX*. 2019 Jan 1;6:2134–40. doi: 10.1016/j.mex.2019.09.015
20. Chinedu E, David A, Fidelis SA. An Approach to Acute, Subacute, Subchronic, and Chronic Toxicity Assessment in Animal Models. *Toxicol Int*. 2015;22(2):83–7. doi: 10.22506/ti/2015/v22/i2/137667
21. Dhiraj Sud, Kumar J, Kaur P, Bansal P. Toxicity, natural and induced degradation of chlorpyrifos. *Journal of the Chilean Chemical Society*. 2020 Jun 1;65(2):4807–16. doi: 10.4067/S0717-97072020000204807
22. Kopjar N, Žunec S, Mendaš G, Micek V, Kašuba V, Mikolić A, et al. Evaluation of chlorpyrifos toxicity through a 28-day study: Cholinesterase activity, oxidative stress responses, parent compound/metabolite levels, and primary DNA damage in blood and brain tissue of adult male Wistar rats. *Chem Biol Interact*. 2018 Jan 5;279:51–63. doi: 10.1016/j.cbi.2017.10.029
23. Bebe FN, Panemangalore M. Exposure to low doses of endosulfan and chlorpyrifos modifies endogenous antioxidants in tissues of rats. *J Environ Sci Health B*. 2003;38(3):349–63. doi: 10.1081/PFC-120019901
24. Noaishi MA, Abd Allah AA, Afify MM. Oral and dermal exposure of chlorpyrifos and cypermethrin mixture induced cytogenetic, histopathological damage and oxidative stress in rats. *J AmSci* 2013;9(3):56-65
25. Pyzik M, Rath T, Kuo TT, Win S, Baker K, Hubbard JJ, et al. Hepatic FcRn regulates albumin homeostasis and susceptibility to liver injury. *Proc Natl Acad Sci U S A*. 2017;114(14). doi: 10.1073/pnas.1618291114
26. Han C, Sheng J, Pei H, Sheng Y, Wang J, Zhou X, et al. Environmental toxin chlorpyrifos induces liver injury by activating P53-mediated ferroptosis via GSDMD-mtROS. *Ecotoxicol Environ Saf*. 2023;257(February):114938. doi: 10.1016/j.ecoenv.2023.114938
27. Su L, Zhang J, Gomez H, Kellum JA, Peng Z. Mitochondria ROS and mitophagy in acute kidney injury. *Autophagy*. 2023;19(2):401–14. doi: 10.1080/15548627.2022.2084862
28. Naime AA, Lopes MW, Colle D, Dafré AL, Suñol C, da Rocha JBT, et al. Glutathione in Chlorpyrifos-and Chlorpyrifos-Oxon-Induced Toxicity: a Comparative Study Focused on Non-cholinergic Toxicity in HT22 Cells. *Neurotox Res*. 2020 Oct 1;38(3):603–10. doi: 10.1007/s12640-020-00254-5
29. Ismail AA, Hendy O, Rasoul GA, Olson JR, Bonner MR, Rohlman DS. Acute and Cumulative Effects of Repeated Exposure to Chlorpyrifos on the Liver and Kidney Function among Egyptian Adolescents. *Toxics*. 2021 Jun;9(6):137. doi: 10.3390/toxics9060137
30. Sakinah EN, Wisudanti DD, Abrori C, Supangat S, Ramadhani LR, Putri IS, et al. The effect of chlorpyrifos oral exposure on the histomorphometric and kidney function in Wistar rat. *Indian J Pharmacol*. 2024;56(3):186–90. doi: 10.4103/ijp.ijp\_820\_23
31. Aung S, Talib AN, Nz A, Z MZ. Mechanism of Chlorpyrifos Induced Chronic Nephrotoxicity Mechanism of Chlorpyrifos Induced Chronic Nephrotoxicity. 2023;(October 2022). doi: 10.31436/imjm.v21i4.2023
32. Benzing T, Salant D. Insights into Glomerular Filtration and Albuminuria. *New England Journal of Medicine*. 2021;384(15):1437–46. doi: 10.1056/NEJMr1808786
33. Kopp JB, Anders HJ, Susztak K, Podestà MA, Remuzzi G, Hildebrandt F, et al. Podocytopathies. *Nat Rev Dis Primers*. 2020;6(1). doi: 10.1038/s41572-020-0196-7
34. Olukiran OS, Akomolafe RO, Ilesanmi OS, Imafidon CE, Alabi QK. Age-related changes in urinary protein excretion in relation to indices of renal function in Wistar rats. *Animal Model Exp Med*. 2018 Dec 1;1(4):295–304. doi: 10.1002/ame2.12035.



# JOURNAL OF BIOMEDICINE AND TRANSLATIONAL RESEARCH

Available online at JBTR website: <https://jbtr.fk.undip.ac.id>

Copyright©2024 by Faculty of Medicine Universitas Diponegoro, Indonesian Society of Human Genetics and Indonesian Society of Internal Medicine

Original Research Article

## Visceral Adiposity Index and Insulin Resistance in Diabetes Mellitus Type 2

Meita Hendrianingtyas<sup>1\*</sup>, Subandhini Arika Pradati<sup>2</sup>

<sup>1</sup>Departement of Clinical Pathology, Faculty of Medicine, Universitas Diponegoro, Indonesia

<sup>2</sup>Faculty of Medicine, Universitas Diponegoro, Indonesia

### Article Info

History

Received: 18 Jun 2024

Accepted: 25 Oct 2024

Available: 30 Dec 2024

### Abstract

**Background:** Central obesity due to visceral fat can cause insulin resistance, risking type 2 diabetes mellitus (DM) with many complications, including coronary heart disease (CHD). The visceral adiposity index (VAI) was developed as a new indicator of visceral fat dysfunction. The gold standard for assessing insulin resistance is the hyperinsulinemia-euglycemia (HEC) clamp. This method is invasive and expensive, so homeostasis model assessment-insulin resistance (HOMA-IR) and quantitative insulin sensitivity check index (QUICKI) are more accessible, practical, and less invasive measurement methods. This study not only analyzed the relationship between VAI and HOMA-IR but also with QUICKI as a marker of insulin resistance.

**Objective:** To determine the correlation between visceral adiposity index and insulin resistance (HOMA IR and QUICKI) in patients with type 2 diabetes mellitus.

**Methods:** A cross-sectional study on 70 adult outpatients with diabetes mellitus in the Diponegoro National Hospital Semarang was performed. Fasting glucose was examined using the hexokinase method, while HDL-C and TG used the colorimetric enzymatic method with an automated clinical chemistry device. Fasting insulin was tested using the Enzyme-Linked Immuno Sorbent Assay (ELISA) method. Weight and height measurement by Tanita body composition scales. VAI, HOMA IR, and QUICKI were calculated manually. Data analysis was performed using the Pearson test ( $p < 0.05$ ).

**Results:** There was a moderate positive correlation between VAI and HOMA-IR ( $r=0.480$ ;  $p<0.001$ ). There was moderate negative correlation between VAI and QUICKI ( $r=-0.475$ ;  $p<0.001$ ).

**Conclusion:** This study shows that the higher the VAI value, the higher the HOMA IR value. Conversely, the higher the VAI value, the lower the QUICKI value. These results indicate that the higher the VAI value, the more severe the insulin resistance in DM patients. Severe insulin resistance can lead to more serious complications in DM.

**Keywords:** Diabetes Mellitus; central obesity; Insulin resistance

**Permalink/ DOI:** <https://doi.org/10.14710/jbtr.v10i3.23505>

### INTRODUCTION

In the last few decades, the prevalence of type 2 diabetes mellitus (DM-T2) has increased throughout the world. In 2015, Indonesia was ranked seventh in the world for the highest prevalence of DM. According to the 2018 Indonesian Ministry of Health Health Research Study, Central Java province has the highest prevalence of type 2 DM.<sup>1</sup>

Diabetes mellitus is a significant risk factor for premature death, and an enormous social and economic

burden. Central obesity is closely related to the high prevalence of T2DM, including acute and chronic complications.<sup>2</sup> High visceral fat in obesity is associated with various systemic diseases including NAFLD, PCOS, hypertension and others.

\*Corresponding author:

E-mail: [meitanote2015@gmail.com](mailto:meitanote2015@gmail.com)  
(Meita Hendrianingtyas)

**Table 1.** Data characteristics of research subjects

Variable	Mean $\pm$ SD	Median (min – max)
Age (year)	56.91 $\pm$ 10.16	
WC (cm)		91.50 (66 – 120)
BMI (kg/m <sup>2</sup> )		25.55 (16.40 – 39.70)
Cholesterol (mg/dL)		200.50 (122 – 346)
LDL-C (mg/dL)	130.04 $\pm$ 52.07	
HDL-C (mg/dL)	43.9 $\pm$ 13.78	
Triglycerides (mg/dL)	158.15 $\pm$ 74.69	
FBS (mg/dL)	155.30 $\pm$ 77.55	
Insulin (IU)	24.05 $\pm$ 37.80	
VAI	9.51 $\pm$ 16.93	
HOMA-IR	0.30 $\pm$ 0.04	
QUICKI	6.50 $\pm$ 3.92	

WC, waist circumference; BMI, body mass index; HDL, high-density lipoprotein- cholesterol; FBS fasting blood sugar; HOMA-IR, homeostasis assessment of insulin resistance; QUICKI, quantitative insulin sensitivity assessment index; VAI, visceral adiposity index; SD(standard deviation); min (minimum); max (maximum).

Individuals with high visceral fat are at increased risk of insulin resistance. A further consequence is that the risk of developing T2DM is also greater.<sup>3</sup> Insulin resistance is a metabolic disorder characterized by the failure of fat storage into subcutaneous adipose tissue, leading to ectopic fat deposition into visceral fat tissue and insulin-sensitive tissues such as liver and skeletal muscle. These tissues progress to lipotoxicity status, interfering with insulin signaling and action, resulting in insulin resistance.<sup>4</sup> The state of insulin resistance in DM patients will cause an increase in further complications such as CHD.<sup>5</sup>

The best measurement of insulin resistance of insulin resistance is using a hyperinsulinemic-euglycemic clamp (HEC), but this method is invasive, time-consuming, and expensive to implement in clinical practice. Current assessment of insulin resistance using the homeostatic model (HOMA-IR) and quantitative insulin sensitivity check index (QUICKI) are more straightforward, practical, and minimally invasive measurement methods. HOMA-IR and QUICKI can be calculated using fasting blood glucose (GDP) and insulin levels.<sup>6</sup> Apart from that, not all laboratories provide parameters for insulin level measurement.

Magnetic resonance imaging (MRI) and computerized tomography scans (CT) can be used to examine visceral fat, which is essential in the mechanism of insulin resistance. However, these techniques are costly, have radiation side effects, and are unavailable in every healthservice. There is a need for a simple alternative parameter to measure visceral fat.<sup>7</sup> The visceral adiposity index (VAI) was developed as a new visceral adipose tissue dysfunction indicator. A previous study reported that VAI can be used to replace visceral CT scan examination as a marker of visceral adiposity. The visceral adiposity index itself is an indirect measurement method based on gender that measures a combination of anthropometric examinations based on waist circumference (WC), body mass index (BMI), triglyceride (TG) levels, and high-density lipoprotein (HDL) cholesterol levels.<sup>7,8</sup> The laboratory's parameters for determining the VAI value are easy and cheap. Almost all laboratories measure all of these parameters.

Previous study reported a correlation between VAI and homeostatic model assessment of insulin resistance (HOMA-IR) in participants with normal weight.<sup>8</sup> Another study showed an increase in VAI and HOMA-IR values in type2 DM patients than control group.<sup>3</sup> The quantitative insulin sensitivity check index is an empirical math-transformed calculation of fasting glucose and plasma insulin levels that has been shown to provide better predictive power consistently and precisely. QUICKI is a variation of the HOMA equation, according to Gutch et al. QUICKI has a better correlation in patients with diabetes and obesity.<sup>6</sup> A cut-off value of HOMA-IR > 2.5 indicates insulin resistance while QUICKI <0.328.<sup>10</sup>

Based on the explanation above, we want to analyze the correlation between VAI and insulin resistance assessed by the HOMA-IR and QUICKI methods in patients with type 2 diabetes mellitus. Previous studies only analyzed VAI and HOMA-IR in DM groups and healthy controls. The difference between this study and several previous studies is that this study not only analyzed the relationship between VAI and HOMA-IR but also with QUICKI as a marker of insulin resistance.

## MATERIALS AND METHODS

A Cross-sectional study on 70 adult diabetes mellitus patients in outpatient care at Diponegoro National Hospital from March to April 2022. Subjects with a history of hepatic, renal, and thyroid disease were excluded from this study. Ethical clearance was obtained from the Health Research Ethics Commission (KEPK) of the Faculty of Medicine, Universitas Diponegoro, with No: 62/EC/KEPK/FK-UNDIP/III/2022.

All subjects agreed to participate in this study by signing an informed consent form. Venous blood was drawn for fasting glucose levels, lipid profiles (cholesterol, HDL, LDL, triglycerides), and insulin levels. They were also subjected to anthropometric examination, including height and weight. A nutritionist took measurements of the height and weight of the study subjects using the Tanita BC tool using Tanita body composition monitor (Tanita Health Equipment H.K. Ltd).

Consecutive sampling will be done according to the research criteria until the number of samples is met. Fasting glucose was examined using the hexokinase method, while HDL-C and TG used the colorimetric enzymatic method with an automated clinical chemistry device (Indiko TM, Thermo Fisher Scientific, Waltham, MA USA). Fasting insulin was tested using the Enzyme-Linked Immuno Sorbent Assay (ELISA) method. Body mass index (BMI) examination calculates of body weight in kg divided by height in meters squared (kg/m<sup>2</sup>). VAI was calculated based on the combination of (WC), (BMI), triglyceride (TG), and (HDL) examinations with the formula<sup>8</sup>:

$$\text{Male: VAI} = \left( \frac{WC}{(39.58 + (1.886 * BMI))} \right) * \left( \frac{TG}{1.03} \right) * \left( \frac{1.31}{HDL} \right)$$

$$\text{Female VAI} = \left( \frac{WC}{(36.58 + (1.896 * BMI))} \right) * \left( \frac{TG}{0.81} \right) * \left( \frac{1.52}{HDL} \right)$$

$$\text{HOMA-IR} = \frac{\text{glucose mg/dL} * \text{insulin } \mu\text{U/L}}{405}$$

$$\text{QUICKI} = \frac{1}{[\log(\text{Insulin } \mu\text{U/mL}) + \log(\text{Glucose mg/dL})]}$$

Numerical data is displayed as mean±SD if the data distribution is normal or median(min-max) if the data distribution is not normal. Test the relationship between VAI with HOMA-IR and QUICKI using the Pearson test (p<0.05).

## RESULT

A total of 70 patients who met the criteria participated in the study. Seventy samples were obtained, consisting of 36 (51,4%) men and 34 (48,6%) women. The distribution of subject characteristics is presented in Table 1. Variables with normal data distributions are shown with the mean±SD, while variables with abnormal data distributions are shown with the median (min-max).

The results of data analysis with the Pearson test showed a moderate positive correlation between the number of VAI and HOMA-IR (p<0.001; r=0.480) and a moderate negative correlation between VAI and QUICKI (p<0.001; r=-0.475) can be seen in table 2.

**Table 2.** Correlation test results of VAI between HOMA-IR and QUICKI

Variable	VAI	
	p	r
HOMA-IR	<0.001	0.480
QUICKI	<0.001	-0.475

The distribution of VAI data with HOMA-IR and QUICKI can be seen in Figure 1 and 2.

## DISCUSSION

There was a positive correlation between VAI and HOMA-IR and a negative correlation between VAI and QUICKI. The correlation between VAI and HOMA-IR is in line with previous research which shows that VAI is closely related to HOMA-IR. This condition can be used

as an independent risk factor influencing the increase in HOMA-IR rates in both male and female groups.<sup>9</sup>

VAI is considered a fat indicator and is essential in managing fat loss. Conventional ways to reduce fat are lifestyle interventions or using medication. This research also showed that obesity is strongly associated with insulin resistance. Those in the BMI >30kg/m<sup>2</sup> group will experience four times more insulin resistance. Increasing TG levels is associated with decreased insulin sensitivity. The lower the HDL-C levels, the more insulin resistance occurs.<sup>11</sup>

Another study on 528 subjects with suspected obstructive sleep apnea with and without obesity and metabolic syndrome, reported that increased VAI was associated with insulin resistance.<sup>12</sup> Study of 439 Bangladeshi population, reported VAI had a positive correlation with HOMA-IR in patients with Type 2 DM but did not show a significant correlation in controls.<sup>3</sup>

A previous study showed that visceral fat has a link with insulin resistance calculated by HOMA IR and QUICKI and metabolic syndrome, which has a better correlation in pre-diabetic women and patients with type 2 DM population.<sup>13</sup> Another study by Vizzuso et al. reported a significant correlation between VAI, HOMA-IR, and QUICKI in a population of Caucasian children aged 8-15 years with metabolic syndrome.<sup>14</sup> Another study concluded a moderate correlation between VAI, HOMA-IR, and QUICKI in 396 obese children in Mexico.<sup>15</sup>

Previous studies have demonstrated the correlation between visceral adipose tissue and insulin resistance. A meta-analysis study by Zhang et al. reported a significant positive association between adipose tissue build-up and insulin resistance as measured by HOMA-IR. The visceral fat mass is closely correlated with HOMA-IR, followed by total fat mass, BMI, and WC.<sup>7</sup>

Sun et al. said there is a correlation between visceral fat in several measurement methods and the risk of diabetes and insulin resistance.<sup>3</sup> Borel et al. showed that changes in visceral adipose tissue were associated with improved insulin sensitivity after one year of lifestyle intervention.<sup>15</sup> The increase influenced the increase in VAI values in WC, BMI, and TG levels. This condition supports the theory that increased fat, especially visceral fat and dyslipidemia, increases glucose blood levels due to insulin resistance. An increased risk of diabetes may result from excess visceral fat. Visceral fat has more excellent endocrine activity than subcutaneous fat and is a marker of adipose tissue dysfunction and ectopic fat deposition. These circumstances cause lipotoxicity and insulin resistance in muscle cells, liver, and pancreatic cells that inhibit glucose uptake. Therefore, visceral fat contributes as one of the risk factors for diabetes.<sup>13</sup>

Insulin resistance measurement with HOMA-IR was done more than 15 years ago.<sup>5</sup> HOMA-IR has been observed to have a linear correlation with glucose clamp and minimal model in estimating insulin sensitivity/resistance in various studies in different populations. In contrast, QUICKI is the logarithm of HOMA-IR, which explains its almost perfect correlation with HOMA-IR.<sup>17</sup> This is consistent with this study, where a very strong correlation was found between HOMA-IR and QUICKI. Katz et al., in their study, also mentioned that

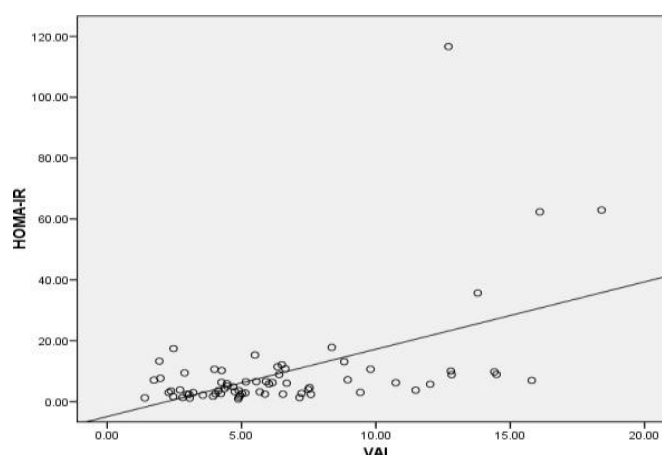


**Figure 1.** Scatter plot graph of Correlation VAI and HOMA-IR

Figure 1 shows the scatter plot of the VAI and HOMA IR relationship. The line in the figure shows a positive correlation between VAI and HOMA IR, i.e., the higher the VAI value, the higher the HOMA IR value. The higher the VAI value, the more severe the state of insulin resistance

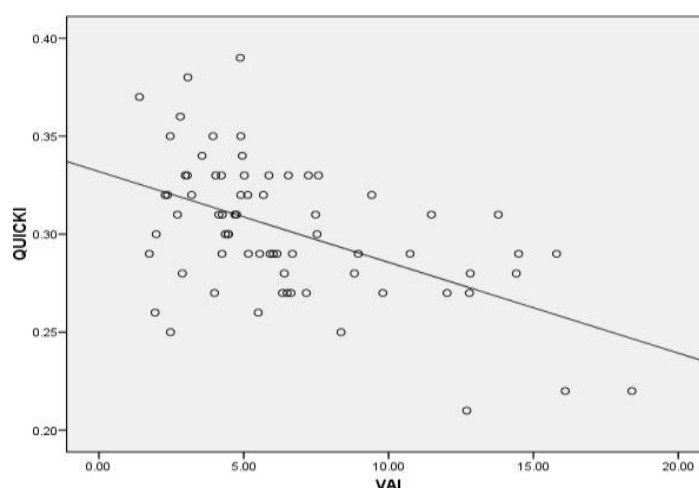


**Figure 2.** Scatter plot graph of VAI correlation with QUICKI

Figure 2 shows the scatter plot of the relationship between VAI and QUICKI. The line in the figure shows a negative correlation between VAI and QUICKI, i.e., the higher the VAI value, the lower the QUICKI value. The higher the VAI value, the more severe the state of insulin resistance.

HOMA-IR and QUICKI have a better correlation than HOMA-IR with glucose clamp.<sup>18</sup>

Insulin resistance occurs due to impaired insulin action in metabolically active tissues and organs, including skeletal muscle, liver, and fat tissue.<sup>13</sup> In insulin resistance, the effect on adipose tissue is an increased hepatic free fatty acid flow that tends to increase hepatic very low-density lipoprotein (VLDL) production. At the same time, ketogenesis remains suppressed due to compensatory hyperinsulinemia.<sup>9</sup> Fat-induced insulin resistance, where there is decreased fat storage capacity within the subcutaneous adipose tissue, will lead to ectopic fat deposition into visceral fat tissue and insulin-sensitive tissues such as liver and skeletal muscle. These tissues will progressively develop to lipotoxicity status, disrupt insulin signaling and action, and cause insulin resistance and decreased glucose tolerance. Insulin resistance increases as BMI, WC, and especially waist-

hip ratio increases. This reflects an increase in adiposity and incredibly visceral adipose tissue.<sup>2,19</sup>

The visceral adiposity index was developed as a novel indicator of visceral adipose tissue dysfunction that proved to be a good indicator of endocrine dysfunction and low-grade inflammation of adipose tissue in a state referred to as adipose tissue dysregulation.<sup>20</sup> Adipose tissue dysregulation altered fat distribution and function and is believed to be a cornerstone in the pathogenesis of insulin resistance through altered adipocytokine production, increased lipolytic activity, and inflammation.<sup>21</sup> Other studies have shown a relationship between obesity parameters and lipid profiles in the form of lipid accumulation products, inflammatory conditions, and glucose levels.<sup>22</sup>

The results of this study indicate that VAI values obtained from examining lipid profile levels (triglycerides and HDL-cholesterol) can be used to assess the state of insulin resistance. This parameter makes it easier for

patients to control further insulin-resistant states. This study did not analyze the length of time the subject suffered from DM. Further research is needed on DM patients and on the period of time after the patient is diagnosed with DM.

## CONCLUSION

This study has a positive correlation between the number of VAI and HOMA-IR and a negative correlation between VAI and QUICKI. The higher VAI value indicates a more severe insulin-resistant state, as seen from the increasing HOMA IR and decreasing QUICKI. The higher the VAI value, the more severe the state of insulin resistance, which can increase complications in DM. Further studies linking VAI and insulin resistance to DM complication parameters are needed.

## REFERENCES

1. Wireno EHD, Setiawan AA, Hendrianingtyas M, Pramudo SG. Factors Affecting Glycemic Control in Diabetes Mellitus Patients. *Sains Med J Kedokt dan Kesehat*. 2021;12(2). Available from: <http://dx.doi.org/10.30659/sainsmed.v12i2.7620>
2. Sun K, Lin D, Feng Q, Li F, Qi Y, Feng W, et al. Assessment of adiposity distribution and its association with diabetes and insulin resistance: A population-based study. *Diabetol Metab Syndr*. 2019;11(1):1–10. Available from: <https://doi.org/10.1186/s13098-019-0450-x>
3. Parveen S, Ayub TE, Haq T, Nahar N, Manbub N, Islam F, et al. Association of visceral adiposity index with insulin resistance in adults with diabetes mellitus. *IMC J Med Sci*. 2020;14(1):5–12.
4. Chen C, Xu Y, Guo ZR, Yang J, Wu M, Hu XS. The application of visceral adiposity index in identifying type 2 diabetes risks based on a prospective cohort in China. *Lipids Health Dis*. 2014;13(1):1–8.
5. Ormazabal V., Nair S., Elfeky O. et al. Association between insulin resistance and the development of cardiovascular disease. *Cardiovasc Diabetol* 17, 122 (2018). <https://doi.org/10.1186/s12933-018-0762-4>.
6. Gutch M, Kumar S, Razi SM, Gupta K, Gupta A. Assessment of insulin sensitivity/resistance. *Indian J Endocrinol Metab*. 2015;19(1):160–4.
7. Zhang M, Zheng L, Li P, Zhu Y, Chang H, Wang X, et al. 4-year trajectory of visceral adiposity index in the development of type 2 diabetes: A prospective cohort study. *Ann Nutr Metab*. 2016;69(2):142–9.
8. Dieny FF, Jauharany FF, Tsani AFA, Fitranti DY. Peningkatan visceral adiposity index berhubungan dengan sindrom metabolik remaja obesitas. *J Gizi Klin Indones*. 2020;16(4):143.
9. Ji B, Qu H, Wang H, Wei H, Deng H. Association between the Visceral Adiposity Index and Homeostatic Model Assessment of Insulin Resistance in Participants with Normal Waist Circumference. *Angiology*. 2017;68(8):716–21.
10. Donma MM, Donma O, Topçu B, Aydın M, Tülübaş F, Nalbantoğlu B, et al. A New Insulin Sensitivity Index Derived From Fat Mass Index and Quantitative Insulin Sensitivity Check Index. 2015;3(1):26–36.
11. Bermúdez V, Salazar J, Fuenmayor J, Nava M, Ortega Á, Duran P, et al. Lipid Accumulation Product Is More Related to Insulin Resistance than the Visceral Adiposity Index in the Maracaibo City Population, Venezuela. *J Obes*. 2021;2021:5514901. doi: 10.1155/2021/5514901
12. Mazzuca E, Battaglia S, Marrone O, Marotta AM, Castrogiovanni A, Esquinas C, et al. Gender-specific anthropometric markers of adiposity, metabolic syndrome and visceral adiposity index (VAI) in patients with obstructive sleep apnea. *J Sleep Res*. 2014;23(1):13–21.
13. Yi W, Kim K, Im M, Ryang S, Kim EH, Kim M, et al. Association between visceral adipose tissue volume, measured using computed tomography, and cardio-metabolic risk factors. *Sci Rep [Internet]*. 2022;12(1):1–8. Available from: <https://doi.org/10.1038/s41598-021-04402-5>
14. Vizzuso S, Del Torto A, Dilillo D, Calcaterra V, Di Profio E, Leone A, et al. Visceral adiposity index (VAI) in children and adolescents with obesity: No association with daily energy intake but promising tool to identify metabolic syndrome (MetS). *Nutrients*. 2021;13(2):1–15.
15. Hernández MJG, Klünder M, Nieto NG, Alvarenga JCL, Gil JV, Huerta SF, et al. Pediatric Visceral Adiposity Index Adaptation Correlates With Homa-Ir, Matsuda, And Transaminases. *Endocr Pract*. 2018;24(3):294–301.
16. Borel AL, Nazare JA, Smith J, Almérás N, Tremblay A, Bergeron J, et al. Improvement in insulin sensitivity following a 1-year lifestyle intervention program in viscerally obese men: Contribution of abdominal adiposity. *Metabolism*. 2012;61(2):262–72.
17. Farkas, G.J.; Gordon, P.S.; Trewick, N.; Gorgey, A.S.; Dolbow, D.R.; Tiozzo, E.; Berg, A.S.; Gater, D.R., Jr. Comparison of Various Indices in Identifying Insulin Resistance and Diabetes in Chronic Spinal Cord Injury. *J. Clin. Med*. 2021, 10, 5591. <https://doi.org/10.3390/jcm10235591>.
18. Žarković M, Ćirić J, Beleslin B, Stojković M, Savić S, Stojanović M, Lalić T. Variability of HOMA and QUICKI insulin sensitivity indices. *Scand J Clin Lab Invest*. 2017 ;77(4):295–7. doi: 10.1080/00365513.2017.1306878.
19. Baveicy K, Mostafaei S, Darbandi M, Hamzeh B, Najafi F, Pasdar Y. Predicting metabolic syndrome by visceral adiposity index, body roundness index and a body shape index in adults: A cross-sectional study from the Iranian ranced cohort data. *Diabetes, Metab Syndr Obes Targets Ther*. 2020;13:879–87.
20. Štěpánek L, Horáková D, Cibičková L, Vaverková H, Karásek D, Nakládalová M, et al. Can visceral adiposity index serve as a simple tool for identifying individuals with insulin resistance in daily clinical practice? *Med*. 2019;55(9).
21. Bijari M, Jangjoo S, Emami N, Raji S, Mottaghi M, Moallem R, et al. The Accuracy of Visceral Adiposity Index for the Screening of Metabolic Syndrome: A Systematic Review and Meta-Analysis. *Int J Endocrinol*. 2021;2021.

- 
22. Surohadi, N.D., Retnoningrum, D., Hendrianingtyas, M., Noer, E.R. and Syauqi, A. 2023. Correlation between Lipid Accumulation Product with Fasting Blood Glucose and CRP in Obese Females. Indonesian Journal Of Clinical Pathology And Medical Laboratory. 2023, 29(1):11–14.  
DOI:<https://doi.org/10.24293/ijcpml.v29i1.1964>.
-